Atmospheric Environment 262 (2021) 118629

Contents lists available at ScienceDirect

Atmospheric Environment

journal homepage: www.elsevier.com/locate/atmosenv

Contribution of AOD-$PM_{2.5}$ surfaces to respiratory-cardiovascular hospital events in urban and rural areas in Baltimore, Maryland, USA: New analytical method correctly identified true positive cases and true negative controls

John T. Braggio [a,e,*], Eric S. Hall [b], Stephanie A. Weber [c,f], Amy K. Huff [d,g]

[a] Maryland Department of Health, Baltimore, MD, 21201, USA
[b] U.S. Environmental Protection Agency, Research Triangle Park, NC, 27709, USA
[c] Battelle Memorial Institute, Columbus, OH, 43201, USA
[d] Battelle Memorial Institute, Arlington, VA, 22201, USA
[e] Mt. Diablo Analytical Solutions and Reporting Institute (Diablo Analytical Institute), 3474 Tice Creek Drive, Unit 7, Walnut Creek, CA, 94595, USA
[f] Huntington National Bank, Columbus, OH, 43215, USA
[g] IMSG at NOAA/NESDIS Center for Satellite Applications and Research, 5825 University Research Ct, Suite 3250, College Park, MD, 20740, USA

HIGHLIGHTS

- Accuracy of respiratory-cardiovascular case-control evaluated in AOD-$PM_{2.5}$ study.
- OR method overestimated true positive cases and correctly detected true negative controls.
- The New Beta algorithm accurately detected true positive cases and true negative controls.
- The new method confirmed the correct classification cases and controls in urban and rural areas.

GRAPHICAL ABSTRACT

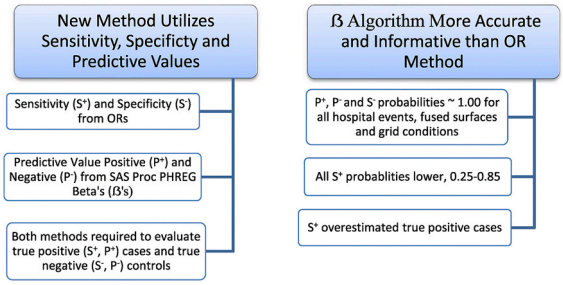

ARTICLE INFO

Keywords:
AOD-$PM_{2.5}$
Respiratory-cardiovascular

ABSTRACT

Epidemiologic studies have used aerosol optical depth (AOD)-$PM_{2.5}$ as a proxy for ambient $PM_{2.5}$ in urban and rural areas, even though its validation with air monitors has only occurred in urban areas. The contribution of

Abbreviations: AIC, Akaike information criterion; AOD, aerosol optical depth; AT, apparent temperature; ß, linear predictor; CI, 95% confidence interval; CLR, conditional logistic regression; CMAQ, Community Multiscale Air Quality Model; ΔOR%, difference OR percent; Dx, disease; ED, emergency department; FN, false negative; FP, false positive; GIS, geographic information system; HBM, hierarchical Bayesian model; HF, heart failure; HSCRC, Maryland Health Services Cost Review Commission; ICD-9-CM, International Classification of Diseases, 9th Revision, Clinical Modification; IP, inpatient; MDH, Maryland Department of Health; MI, myocardial infarction; OR, odds ratio; $PM_{2.5}$, fine particulate matter ≤2.5 μm; PMB, monitor $PM_{2.5}$ and CMAQ $PM_{2.5}$; PMC, monitor $PM_{2.5}$ and AOD-$PM_{2.5}$ not-Kriged; PMCK, monitor $PM_{2.5}$ and AOD-$PM_{2.5}$ Kriged; PMCKQ, monitor $PM_{2.5}$, AOD-$PM_{2.5}$ Kriged and CMAQ $PM_{2.5}$; PMCQ, monitor $PM_{2.5}$, AOD-$PM_{2.5}$ not-Kriged and CMAQ $PM_{2.5}$; P^+, predictive value positive; P^-, predictive value negative; S^+, sensitivity; S^-, specificity; SE, standard error; TN, true negative; TP, true positive; ZCTA, ZIP code tabulation area; ZIP, zone improvement plan.

* Corresponding author. Diablo Analytical Solutions and Reporting Institute (Diablo Analytical Institute), 3474 Tice Creek Drive, Unit 7, Walnut Creek, CA 94595, USA.

E-mail addresses: johntbs@msn.com (J.T. Braggio), hall.erics@epa.gov (E.S. Hall), stephanieaweber@gmail.com (S.A. Weber), amy.huff@noaa.gov (A.K. Huff).

https://doi.org/10.1016/j.atmosenv.2021.118629
Received 2 March 2021; Received in revised form 27 June 2021; Accepted 17 July 2021
Available online 22 July 2021

True positive/negative
Sensitivity/ specificity
Predictive value positive/negative
Rural-urban

elevated AOD-$PM_{2.5}$ on respiratory-cardiovascular true positive (TP) cases, exposed to high $PM_{2.5}$, and true negative (TN) controls, not exposed to elevated $PM_{2.5}$, was evaluated in 72 Community Multiscale Air Quality (CMAQ) grids with (urban) and without (rural) air monitors. The odds ratio (OR) algorithm and the newly developed beta (ß) algorithm were used to evaluate the reliability and validity of TP cases, and TN controls in grids with and without air monitors. Four experimental AOD-$PM_{2.5}$ fused surfaces and four health outcomes were evaluated. Only the linear predictor (ß) algorithm reliably and correctly identified TP cases and TN controls, with probabilities ~1.00. The OR algorithm only identified TN controls, with probabilities ~1.00, and significantly overestimated the percentage of TP cases. Regression analyses demonstrated that the OR algorithm's accuracy could be improved if the number of cases for all health outcomes was increased 50.8% in all grids and 73.9% in grids without monitors. Since the number and percentage of TP cases and TN controls were similar in grids with and without air monitors, this outcome suggests that the AOD-$PM_{2.5}$ and health outcome concentration-response function evaluated in grids with monitors also holds in grids without air monitors. The possible use of AOD-$PM_{2.5}$ fused surfaces, as another epidemiologic tool, to assess elevated ambient $PM_{2.5}$ concentration levels to respiratory-cardiovascular hospital events in rural areas is discussed.

1. Introduction

Published studies have found robust correlations, or other statistical measures of association, between variations in aerosol optical depth (AOD) unitless values and similar changes in ambient PM $\leq$ 2.5 ($PM_{2.5}$) monitor concentration levels in urban areas where, in the United States, there are on-the-ground ambient air monitors (Belle and Liu, 2016; Chang et al., 2014; Christopher and Gupta, 2020; Chu et al., 2016; Di et al., 2019; Engel-Cox et al., 2004; Fu et al., 2020; Geng et al., 2018; Guo et al., 2009; Hu, 2009; Hu et al., 2014; Jin et al., 2020; Kloog et al., 2012b, 2014a; Kumar et al., 2007; Lee et al., 2012; Lee et al., 2016a; Li et al., 2015; Liu et al., 2005; Ma et al., 2016; van Donkelaar et al., 2010, 2015; Vu et al., 2019; Wang and Chen, 2016; Weber et al., 2010; Xie et al., 2019; Xue et al., 2017; Yanosky et al., 2014; Zhang et al., 2009). Satellite AOD and monitor $PM_{2.5}$ validation studies have been rarely undertaken in rural areas because of the absence of air monitors (Bell and Ebisu, 2012; Fu et al., 2020; Geng et al., 2018; Hu et al., 2014; Lee et al., 2016a, 2016b).

Another research direction is the evaluation of the contribution of AOD-$PM_{2.5}$ concentration levels for selected health outcomes, such as respiratory-cardiovascular emergency department (ED) visits, inpatient (IP) hospitalizations, and mortality (Cordova et al., 2020; Hu, 2009; Hu and Rao, 2009; Khalili et al., 2018; Kloog et al., 2012a, 2014b; Kumar et al., 2013; Lee et al., 2016b; Liu et al., 2016; Madrigano et al., 2013; McGuinn et al., 2016; Prud'homme et al., 2013; Strickland et al., 2016; Tapia et al., 2020; Tétreault et al., 2016). AOD-$PM_{2.5}$ and health outcome studies have found significant odds ratios (ORs), thereby suggesting that these proxies for elevated ambient $PM_{2.5}$ values contribute to the subsequent occurrence of adverse health outcomes. Results from ambient $PM_{2.5}$ monitor studies and respiratory-cardiovascular health outcomes are in agreement with the results from AOD-$PM_{2.5}$ and respiratory-cardiovascular health outcomes, including mortality (Amsalu et al., 2019; Argacha et al., 2016; Babin et al., 2008; Brook and Kousha, 2015; Chen et al., 2016; Cheng et al., 2014; Dai et al., 2018; Garcia et al., 2019; Gehring et al., 2015; Gong et al., 2019; Kim et al., 2017; Ma et al., 2019; Norris et al., 1999; Peters et al., 2001; Qui et al., 2013; Rodopoulou et al., 2015; Szyszkowicz et al., 2018; Tsai et al., 2013; Wang et al., 2017, 2019; Wu et al., 2019; Xia and Yao, 2019; Yu et al., 2018, 2020). These studies included a mixture of urban and rural areas combined into one large study site. Results for urban areas may resemble similar outcomes for rural areas (Lee et al., 2016a; 2016b; Prud'homme et al., 2013). Taken together, these different sources of evidence support, in general, the premise that the AOD-$PM_{2.5}$ association that was only confirmed in urban areas with monitors, could also describe the same relationship in rural areas, even in the absence of air monitor validation studies (Fu et al., 2020; Han et al., 2020; Lee et al., 2016a, 2016b; Prud'homme et al., 2013; Sorek-Hamer et al., 2016).

This study took a different approach to the validation of the relationship between AOD-$PM_{2.5}$ and selected health outcomes by utilizing an analysis of true positive (TP) cases, and true negative (TN) controls (Agresti, 2002; Altman and Bland, 1994a, 1994b; Armitage et al., 2002; German, 2000; Hennekens and Buring, 1987; Hughes, 2017; Kumar, 2016; Last, 1995). Patients exposed to elevated AOD-$PM_{2.5}$ concentration levels and who demonstrate a chronic disease (Dx) are identified as TP cases. In contrast, matched patients not exposed to high AOD-$PM_{2.5}$ concentration levels and do not show a Dx are referred to as TN controls.

The first study objective was to utilize the currently available OR algorithm and the newly developed ß algorithm to detect TP cases and TN controls in grids with air monitors, in grids without air monitors, and in all grids. Medical epidemiologists have used sensitivity (S^+)/predictive value positive (P^+) probabilities to evaluate the reliability and accuracy of TP cases, and specificity (S^-)/predictive value negative (P^-) probabilities to assess the reliability and validity of TN controls (Agresti, 2002; Altman and Bland, 1994a, 1994b; Armitage et al., 2002; German, 2000; Hennekens and Buring, 1987; Hughes, 2017; Kelsey et al., 1996; Kumar, 2016; Last, 1995; Schlesselman, 1982). However, up to now, S^+/S^- and P^+/P^- probability analyses have not been used to validate TP cases and TN controls in environmental epidemiologic studies such as this one, which evaluated the effects of elevated AOD-$PM_{2.5}$ concentration levels on respiratory-cardiovascular chronic disease ED visits and IP hospitalizations (Braggio et al., 2020).

The second objective was to utilize the results for TP cases, and TN controls in grids with and without air monitors to evaluate the assumption about the concentration-response function between AOD-$PM_{2.5}$ and selected respiratory-cardiovascular ED visits and IP hospitalizations developed in grids with monitors is also applicable in grids without air monitors. Confirmatory evidence would be similar in the number and percentage of TP cases and TN controls in grids with and in grids without air monitors. This outcome, if it does occur, would provide additional support for the currently held position that it is possible to utilize AOD-$PM_{2.5}$ fused surfaces in rural areas to more fully evaluate the occurrence of respiratory-cardiovascular hospital events that result from exposure to elevated ambient $PM_{2.5}$ concentration levels (Lee et al., 2016a, 2016b; Prud'homme et al., 2013; Sorek-Hamer et al., 2016).

2. Materials and Methods

The recently published Braggio and associates (2020) study described the methods used to compile and analyze the four concatenated AOD-$PM_{2.5}$ fused surfaces and respiratory-cardiovascular hospital event files, one each for ED asthma visits, and IP asthma, myocardial infarction (MI), and heart failure (HF) hospitalizations. This section will include additional information relevant to how the OR case and Beta (ß) case groups were formed and how the S^+/S^- and P^+/P^- probability analyses were undertaken. Other issues in the Braggio and associates (2020) Baltimore study area publication and the Weber et al. (2016) New York City study area paper will only appear in summary. However, the issues are essential to the understanding of the objectives and outcomes of this study. The Maryland Department Health MDH (2021) Institutional Review Board and the Maryland Health Services Cost

Review Commission (HSCRC, 2020) approved this study.

2.1. Baltimore study area

The Baltimore study area is shown in the Maryland choropleth map, Fig. 1, below,

consisted of 99 12 km^2 Community Multiscale Air Quality (CMAQ) grids (EPA, 2020a). However, with available health data, the study area was limited to 72 of the 99 grids. The excluded grids did not include out-of-state areas and some Maryland counties: 12 grids in the neighboring State of Pennsylvania; 7 in the District of Columbia and Virginia; and 8 over water in the Chesapeake Bay. The Baltimore study area included Baltimore City and 13 Maryland Counties: Anne Arundel, Baltimore, Calvert, Carroll, Cecil, Frederick, Harford, Howard, Kent, Montgomery, Prince George's, Queen Anne's, and Talbot. Total residents in these 14 jurisdictions represented 87.1% (5,026,895) of the State's 2010 population (5,773,552). The 17 Federal Reference Method ambient $PM_{2.5}$ air monitors are displayed as red hue triangles in Fig. 1. The six jurisdictions with on-the-ground ambient fine PM air monitors (Anne Arundel (4 monitors), Baltimore (2), Baltimore City (6), Harford (1), Montgomery (1), Prince George's (3)) had 80.4% (4,043,669) of the population in Baltimore study area. In contrast, the 8 Counties without air monitors only included 19.6% (983,226) of the population. The counties shown in pale yellow hue provided the 2004–2006 ED visits and IP hospitalizations obtained from the Maryland HSCRC (2020). The green circles represent the centroids for the 99 CMAQ 12 km^2 grids (1–11 rows, south to north, and 1–9 columns, west to east) for Maryland, Pennsylvania, Virginia, and Washington, DC.

2.2. Study flow chart

It was necessary to complete a multi-step data analysis protocol to quantify TP cases and TN controls for the baseline and the four AOD-$PM_{2.5}$ surfaces. Fig. 2 displays the data formatting and data analysis steps. These data analysis steps included the linking of each of the five exposure surfaces with the four health outcome files (1), using the case-crossover design to analyze the 20 different linked exposure-health data files (2), completing 60 conditional logistic regression runs for all grids (20), grids with (20) and grids without (20) ambient air monitors (3), inspecting the statistical analyses from the conditional logistic regression (CLR) runs (4) and computing TP cases and TN controls for the OR and ß algorithms for all for the entire Baltimore study area and in urban grids with ambient air monitors and in rural grids without ambient air monitors (5). Each of the five flow chart steps also identified specific sections in the Materials and Methods section of this paper that provided more detailed information about each data analysis procedure.

2.3. AOD-$PM_{2.5}$ and PMB fused surfaces

Bayesian statistical methods were utilized to combine the different input surfaces to produce the four experimental AOD-$PM_{2.5}$ fused surfaces and the currently used baseline (PMB) fused surface (Braggio et al., 2020; Foley et al., 2010; Hall, 2018; McMillan et al., 2010; Weber et al., 2010, 2016). Forming the five fused surfaces was accomplished by first updating a previously developed hierarchical Bayesian model (HBM) that could only combine two fused surfaces to accept three input surfaces, with either complete or missing observations.

The four AOD-$PM_{2.5}$ fused surfaces utilized daily AOD readings that came from two satellites' recording columns. The columns extended from the satellites' location in outer space to the surface of the earth (Braggio et al., 2020; Weber et al., 2016). The Aqua satellite made AOD readings in the morning. The Terra satellite made AOD readings in the afternoon. Because of cloud cover interference and possible AOD recording failures, the raw AOD data files had missing observations. Missing AOD readings were minimized by using duplicate daily AOD readings from the two satellites. When both satellites had missing AOD readings on the same day, the combined AOD output file also had missing data.

We utilized the updated HBM to generate the four experimental AOD-$PM_{2.5,}$ and PMB fused surfaces (Braggio et al., 2020; Foley et al.,

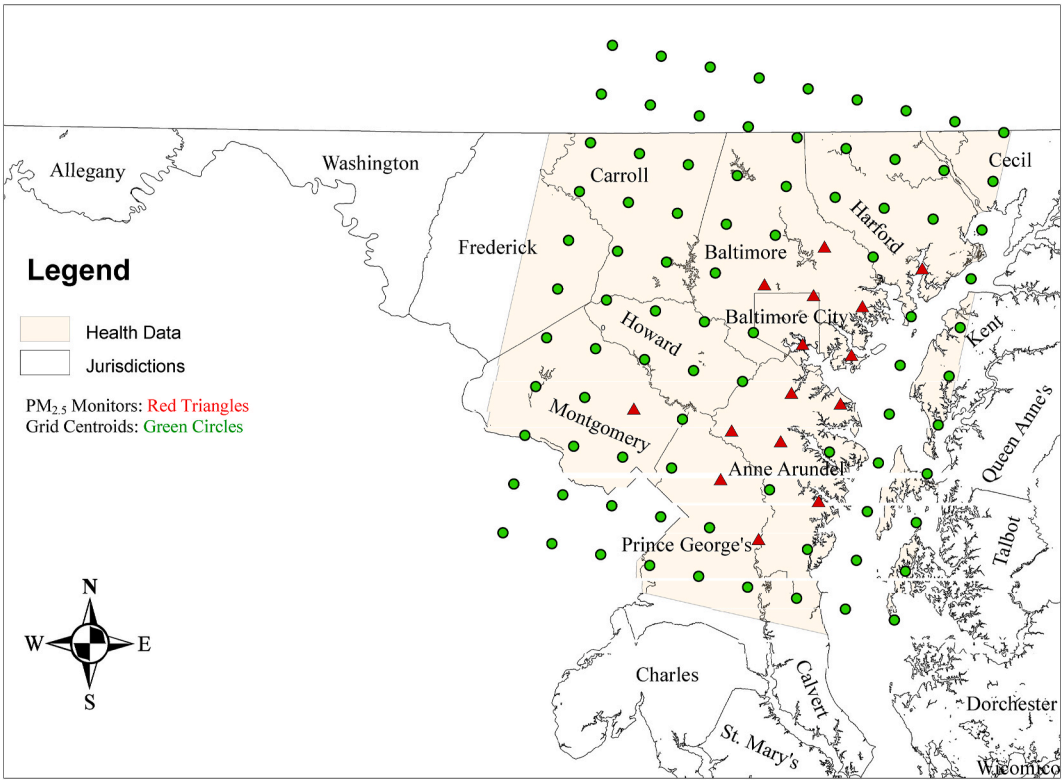

Fig. 1. Maryland choropleth map showing the Baltimore study area.

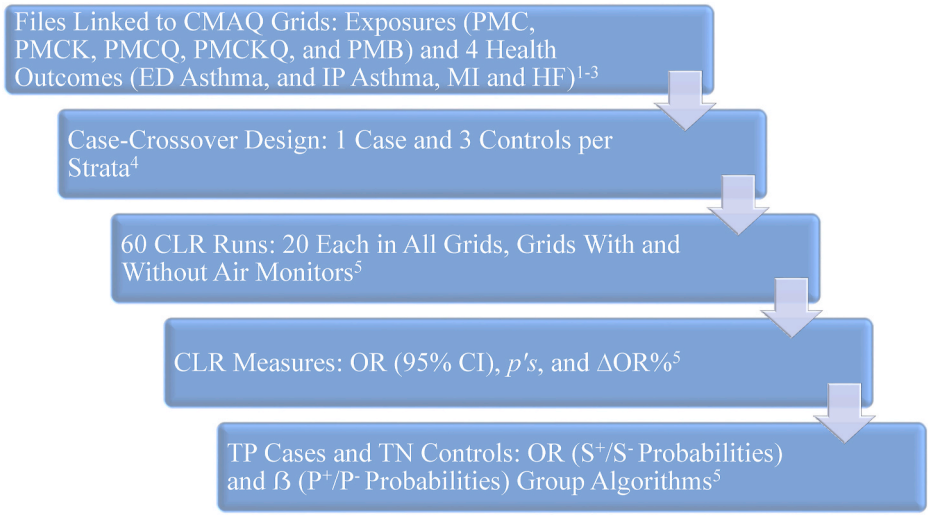

Fig. 2. Flow chart shows the data compilation and analysis steps that were followed to link the exposure and the health outcome files, complete conditional logistic regression (CLR) runs, and determine True Positive (TP) cases and True Negative (TN) controls for the OR and the newly developed ß algorithms. Additional information for each of the 5 steps is given in these Materials and Methods sections: [1]AOD-$PM_{2.5}$ and PMB fused surfaces (2.3), [2]ED visits and IP hospitalizations (2.4), [3]File Linkage (2.6), [4]Case-crossover analyses (2.7), [5]CLR runs (2.8), and [5]TP cases and TN controls for the OR (S^+/S^-) and ß (P^+/P^-) algorithms (OR and ß algorithms, 2.9; S^+/S^- and P^+/P^- probability analyses, 2.10).

2010; Hall, 2018; McMillan et al., 2010; Weber et al., 2010, 2016). Ordinary Kriging was used to eliminate missing AOD daily observations in the combined AOD file (Braggio et al., 2020; Weber et al., 2016). Then, the AOD readings were converted to $PM_{2.5}$ concentration levels by applying a previously developed algorithm (Braggio et al., 2020; Weber et al., 2010, 2016).

Each experimental AOD-$PM_{2.5}$ and PMB fused surface was formed by combing ambient $PM_{2.5}$ air monitor readings (EPA, 2020a), AOD-$PM_{2.5}$ concentration level files that had (not-Kriged) or did not have (Kriged) missing AOD-$PM_{2.5}$ calibrated readings, with or without CMAQ version 4.7 $PM_{2.5}$ model predictions (EPA, 2020b; Foley et al., 2010). By using pre-established combinations of these four $PM_{2.5}$ input files, it was possible to produce four different AOD-$PM_{2.5}$ fused surfaces and also to update the previously developed PMB: 1) The first AOD-$PM_{2.5}$ fused surface, which was named PMC, included ambient $PM_{2.5}$ air monitor readings with the not-Kriged AOD-$PM_{2.5}$ values (i.e., this output file contained missing AOD-$PM_{2.5}$ readings); 2) PMCK included ambient $PM_{2.5}$ air monitor readings with the AOD-$PM_{2.5}$ Kriged surface values (i.e., this output file had no missing AOD-$PM_{2.5}$ readings). The other two fused surfaces had CMAQ $PM_{2.5}$ model predictions: 3) PMCQ was formed by combing ambient $PM_{2.5}$ air monitor readings, PMC readings (not-Kriged), and CMAQ $PM_{2.5}$ model predictions; and 4) PMCKQ included ambient $PM_{2.5}$ air monitor readings, PMCK (Kriged) and CMAQ $PM_{2.5}$ model predictions. 5) PMB was updated for the Baltimore study area (Braggio et al., 2020). PMB included ambient $PM_{2.5}$ air monitor readings with CMAQ $PM_{2.5}$ model predictions. PMB did not include AOD-$PM_{2.5}$ observations. The HBM gave more weight to ambient $PM_{2.5}$ monitor readings in CMAQ grids with at least one ambient air monitor for the PMB fused surface. In CMAQ grids without a single air monitor, the HBM gave more weight to the CMAQ $PM_{2.5}$ model predictions over the $PM_{2.5}$ monitor readings.

2.4. ED visits and IP hospitalizations

The 2004–2006 HSCRC electronic patient records for the four respiratory-cardiovascular chronic diseases were selected from the ambulatory (ED visits) and IP files by using the International Classification of Diseases, 9th revision, Clinical Modification (ICD-9-CM) codes (CDC, 2020) in the primary diagnosis field: asthma (493), MI (410), and HF (428). In addition, co-morbid conditions were also identified by using the ICD-9-CM codes entered in the secondary diagnosis fields: diabetes mellitus (250), hypertension (401), and atherosclerosis (414, 440).

2.5. Confounders

Variables included in the CLR runs were previously shown to influence respiratory-cardiovascular chronic disease ED visits and IP hospitalizations independently. Pollen readings were obtained from the single pollen counting station in Baltimore County, Maryland (Braggio et al., 2012, 2020). Pollen readings were available during the annual pollen season, which started in March and ended in October. Federal holidays (and the day after; OPM, 2020) and snowstorms (NCEI, 2020) were entered as dummy variables (0 = No, 1 = Yes). Apparent temperature (AT) and AT^2 were used to control for the effects of experienced ambient temperature, as influenced by relative humidity and wind speed. These weather data were obtained from the CMAQ version 4.7 model (EPA, 2020a) and made available to the Baltimore investigators by a co-author (ESH). AT was computed using the formula reported on the National Oceanic and Atmospheric Administration website (Braggio et al., 2020; Haley et al., 2009; NOAA, 2020; Rothfusz, 2020; Weber et al., 2016).

2.6. File linkage

We utilized a geographic information system (GIS) to develop a spatial polygon correspondence file that assigned each zone improvement plan (ZIP) code polygon, with its associated respiratory-cardiovascular chronic disease ED visit or IP hospitalization record, to one 12 km^2 CMAQ grid (Braggio et al., 2014; ESRI, 2020). ZIP code latitude-longitude coordinates were entered in the GIS, including the 11 south-north by 9 west-east CMAQ 12 km^2 grid overlay for the Baltimore study area. Next, the ZIP code latitude-longitude coordinates for each polygon were mapped to one CMAQ 12 km^2 grid (MDP, 2020). This 1:1 mapping necessitated selecting only one CMAQ grid that contained the ZIP code's coordinates within the grid's boundaries. The identified unique CMAQ grid coordinate ID was subsequently associated with the ZIP code ID in the correspondence file (Braggio et al., 2014, 2020). This step was repeated for each State's 489 ZIP codes and separately for each of the three years, 2004–2006. After completing this step, the three files, one for each year, were merged into a single multi-year 2004–2006 file. This exact procedure was implemented to identify a single CMAQ grid ID for each ZIP code tabulation area (ZCTA) polygon. These ZCTA polygons included demographic information about population density and poverty (USCB, 2020). File linkage of the various health outcome (ZIP codes) and demographic (ZCTAs) data files was accomplished by merging all data files on the CMAQ grid identifiers for the spatial location variable (1–11 rows, 1–9 columns) and years (2004–2006) for the temporal variable by using Base SAS (SAS, 2017). The files were first linked for each of the three years separately and then combined into one

three-year file. This exact procedure was followed for each of the four health outcome files.

2.7. Case-crossover analyses

Braggio and associates (2020) described how the case-crossover design was used to analyze the contribution of the four experimental AOD-$PM_{2.5}$ and PMB fused surfaces to the four respiratory-cardiovascular hospital events (ED asthma, and IP asthma, MI, and HF hospitalizations on lag day 0. The case-crossover design first described by Maclure (1991) was implemented in the Braggio and associates (2020) study that included the four AOD-$PM_{2.5}$ and PMB fused surfaces linked to the four hospital events. The patient cases were also utilized to form the three controls (Stokes et al., 2012). For the cases, the quarterly AOD-$PM_{2.5}$ exposure window for all five fused surfaces was congruent with the hospital event data. For the three controls, a different quarterly AOD-$PM_{2.5}$ exposure interval was selected. One case and three controls were assigned to each stratum. The observation unit was the stratum and not the individual cases and controls. For all strata included in the CLR runs, the temporal order of the different exposure windows for the controls either preceded or followed the temporal order of the cases. For this reason, the type of case-crossover design used in the Braggio, and associates (2020) publication was a bi-direction lag day case-crossover design (Carracedo-Martinez et al., 2010).

2.8. CLR runs

All CLR analyses were restricted to lag day 0, the index day, when the ED visit or IP hospitalization occurred (Braggio et al., 2020; Hosmer et al., 2013; Stokes et al., 2012). The base CLR runs controlled for pollen confounders, major holidays (and the day after), snowstorms, AT, and AT^2. To each base CLR run, one of the four experimental AOD-$PM_{2.5}$ (PMC, PMCK, PMCQ, PMCKQ) and PMB fused surfaces was entered. Five CLR runs, one each for the five fused surfaces, were completed for each of the four respiratory-cardiovascular hospital events. CLR runs were executed for all CMAQ grids and again for grids with and without air monitors. Braggio and associates (2020) described the evaluation of confounders and effect modifiers. The assessment was a multi-step process. During the screening of confounders and effect modifiers, any variable with a $p \leq 0.09$ was retained. In the final CLR runs, effect modifiers were considered necessary if $p \leq 0.05$. All variables in the last CLR runs were also evaluated with the Akaike information criterion (AIC) (Agresti, 2002; Hosmer et al., 2013). Lower AIC values represent a more economical grouping of confounders, effect modifiers, and predictor variables. The final CLR runs utilized in this data analysis study resembled the final CLR runs previously developed by Braggio and associates (2020).

The outcomes of interest obtained from CLR runs were the OR, the level of significance of the OR, and the OR's 95% confidence interval (CI). The essential CLR outcome required to compute S^+/S^- probabilities was the difference OR percent (ΔOR%) measure. These statistical measures were used to calculate S probabilities and determine the number and percentage of TP cases and TN controls (Agresti, 2002). All analyses were completed using Base SAS and the SAS PHREG procedure within the SAS/STAT statistical package (SAS, 2017, 2018). CLR runs also generated output that was required to compute P probabilities for the newly developed ß algorithm. The SAS PHREG Proc OUTPUT file included ß values for each case and each control (SAS, 2018).

The first step in identifying an elevated ß case was to statistically evaluate the difference between the case ß value and the mean ß value and mean standard error (SE) value for the three controls within each stratum. The one-tail 95% CI was computed for the three matched controls (Agresti, 2002). The one tail 95% CI was obtained by multiplying the control mean SE with the Z value of 1.64, equivalent to the one-tail probability of $p = 0.05$. This computed CI value was added to the mean ß value for the three controls to obtain the one-tail, 95% CI upper limit. If the case's ß value was above the control's upper limit, the case was assigned to the elevated ß case group (P^+) in the same stratum. This outcome was equivalent to the identification of a TP case. If the case's ß value did not exceed the control mean's 95% CI upper limit, the case was assigned to the not-elevated ß case group (P^-). This outcome was the same as the detection of a TN control. The ß algorithm analysis was completed for all strata in the input file. For each case and the three matched controls in each stratum, the SAS PHREG procedure OUTPUT file also included information about CMAQ grid location, which was previously coded for each CLR run. It represented a single CMAQ 12 km^2 grid that contained or did not have at least one ambient fine PM air monitor.

The CLR statistical measures necessary to compute S^+/S^- and P^+/P^- probabilities for each of the four experimental AOD-$PM_{2.5}$ and PMB fused surfaces are summarized in Tables S1 (all grids), S2 (grids with ambient $PM_{2.5}$ air monitors), and S3 (grids without ambient $PM_{2.5}$ air monitors) and included in the supplemental file.

2.9. OR and ß algorithms

There are similarities and differences between the two algorithms evaluated in this data analysis study for their effectiveness in identifying TP cases and TN controls. Each algorithm utilizes the ß statistic. The OR algorithm uses the OR statistic, which is computed by exponentiating the OR-associated ß statistic. Any increase in the OR from 1.00 can be expressed as a percentage representing a relative increase in risk. This ΔOR% value can determine the total cases based on the total number of observations (cases and controls). The newly developed ß algorithm evaluates statistical differences between each case's ß and the mean ß value for the three controls within each stratum. A stratum only contributes to the TP case total if the case ß value was significantly higher than the mean ß value for the three controls. When the case ß value was not significantly different from the mean ß value for the three controls, then this outcome added one observation to the TN control total. The most crucial difference between the OR and ß algorithms is that the former procedure identified TP cases and TN controls by utilizing one summary measure (i.e., ΔOR%). At the same time, the latter algorithm evaluated TP cases and TN controls in each stratum.

2.10. S^+/S^- and P^+/P^- probability analyses

Fig. 3 displays the 2 x 2 table used to compute S^+/S^- and P^+/P^- probabilities. In the medical epidemiologic literature (Armitage et al., 2002; Hennekens and Buring, 1987; Last, 1995), the standard terminology is to use Dx to refer to the presence of chronic disease. The "gold standard" refers to the currently used procedure to determine when Dx is present or absent. In this study, the gold standard was the OR case group algorithm. "Test" is the name for the newly developed test procedure used to determine when Dx is present or absent. Following this terminology, "disease (Dx) present" is associated with the OR case elevated (Above, +) outcome, and "Dx absent" is associated with the not-elevated (Below, -) result. Dx present is also related to the ß case elevated (Above, +) outcome, and Dx absent is associated with the ß case not-elevated (Below, -) outcome.

Fig. 3 displays in rows and columns the occurrence of TP cases (top left cell) and TN controls (bottom right cell). In rows, the S^+ probabilities are equivalent to identifying TP cases, and S^- probabilities are equivalent to identifying TN controls (Agresti, 2002). In columns, P^+ probabilities indicate the detection of TP cases (cases > controls) and P^- probabilities identify the occurrence of TN controls (cases = controls). Probability magnitude represents the degree of reliability or confidence in identifying TP cases and TN controls. Reliability values are highest as the probability values approach 1.00. Reliability values decrease as the probability goes down, <1.00.

The critical concept that underlies the computation of S and P probabilities is that S^+/S^- probabilities are dependent on P^+/P^-

		ß Case (Test)		Total[1]
		Above (+)	Below (-)	
OR Case (Dx)	Above (+)	OR^+, $ß^+$ TP (314)	OR^+, $ß^-$ FP **(128)**	$\sum OR^+$ (442)
	Below (-)	OR^-, $ß^+$ FN **(0)**	OR^-, $ß^-$ TN (10,898)	$\sum OR^-$ (10,898)
Total[2]		$\sum ß^+$ (314)	$\sum ß^-$ (11,026)	(11,340)

[1] $\sum OR^+ = (OR^+, ß^+) + (OR^+, ß^-)$; $\sum OR^- = (OR^-, ß^+) + (OR^-, ß^-)$.
[2] $\sum ß^+ = (OR^+, ß^+) + (OR^-, ß^+)$; $\sum ß^- = (OR^+, ß^-) + (OR^-, ß^-)$.

1. True Positive (TP)/Sensitivity (S^+): $P(ß^+|OR^+) = (OR^+, ß^+)/\sum OR^+$.
2. True Negative (TN)/Specificity (S^-): $P(ß^-|OR^-) = (OR^-, ß^-)/\sum OR^-$.
3. TP/Predictive Value Positive (P^+): $P(OR^+|ß^+) = (OR^+, ß^+)/\sum ß^+$.
4. TN/Predictive Value Negative (P^-): $P(OR^-|ß^-) = (OR^-, ß^-)/\sum ß^-$.

Fig. 3. Formulas used to compute true positive (TP) (OR^+, $ß^+$, top-left cell), true negative (TN) (OR^-, $ß^-$, bottom-right), false positive (FP) (OR^+, $ß^-$, top-right) and false negative (FN) (OR^-, $ß^+$, bottom-left) probabilities. The selected numerical example includes results from Table S1, all CMAQ grids, for ED asthma's PMC fused surface. TP case and TN control totals are shown within the parentheses in regular font. FP case and FN control totals are also in parentheses, obtained by subtraction, and are displayed in **bold** font. Only the analysis of TP cases and TN controls is the focus of the results described in this paper. FP cases and FN controls are only shown here to better understand how TP cases and TN controls were computed.

probabilities. Both are required to evaluate the OR case algorithm and the ß case algorithm for the occurrence of TP cases and TN controls (Agresti, 2002). The OR case total for the elevated group is equivalent to the ß case count for the elevated group, and both outcomes appear in the (OR^+, $ß^+$) cell, in the top left row in Fig. 3. This outcome represents the condition when Dx is present (TP case). Likewise, the OR case total for the not-elevated group equals the ß case total for the not-elevated group, and both outcomes appear in the (OR^-, $ß^-$) cell, in the bottom right row. This outcome codes the condition when Dx is absent (TN control). The total in the other two cells is determined by subtraction. The top-right cell represents false positive (FP) cases (controls), and the bottom left cell is equivalent to false negative (FN) controls (cases). Since the purpose of these probability analyses was to reliably and validly (i.e., correctly) identify TP cases and TN controls, minimal description will deal with FP and FN outcomes.

S^+/S^- analyses evaluated the effectiveness of the OR case algorithm to identify TP cases and TN controls correctly. S^+ probability represents the accuracy of the OR case group to correctly identify the elevated OR cases when Dx is present (OR^+, $ß^+$), TP cases. When the high OR case total (OR^+) is greater than the high ß case total ($ß^+$), the additional observations are assigned to the (OR^+, $ß^-$) cell. The S^+ probability value is computed by dividing the sum in the (OR^+, $ß^+$) cell by the total for all elevated OR cases, $\sum OR^+$. The S^- probability represents the accuracy of the OR case group to correctly identify not-elevated OR cases when Dx is absent, TN controls. When the not-elevated OR case total (OR^-) is greater than the not-elevated ß case total ($ß^-$), the additional observations are assigned to the (OR^-, $ß^+$) cell. The S^- probability is computed by dividing the sum in the (OR^-, $ß^-$) cell by the total for not-elevated OR cases, $\sum OR^-$.

P^+/P^- probability analyses assessed the effectiveness of the ß case group algorithm to identify TP cases and TN controls correctly. $ß^+$ probability represents the accuracy of the $ß^+$ case algorithm to correctly identify elevated ß cases when Dx is present (OR^+, $ß^+$), TP cases. When the elevated ß case total ($ß^+$) is greater than the high OR case total (OR^+), the additional observations are assigned to the (OR^-, $ß^+$) cell. The P^+ probability value is computed by dividing the sum in the (OR^+, $ß^+$) cell by the total for all elevated ß cases, $\sum ß^+$. The P^- probability represents the accuracy of the ß case group algorithm to correctly identify the not-elevated ß cases when Dx is absent, TN controls. When the not-elevated ß case total ($ß^-$) is greater than the not-elevated OR case total (OR^-), the additional observations are assigned to the (OR^+, $ß^-$) cell. P^- probability is computed by dividing the sum in the (OR^-, $ß^-$) cell by the total for the not-elevated ß-cases, $\sum ß^-$.

The totals in parentheses, shown in Fig. 3, represent actual observations from Table S1 (supplemental file) for ED asthma, PMC AOD-$PM_{2.5}$ fused surface (2nd row down from the top of the table). The totals for OR^- (10,898), OR^+ (442), $ß^-$ (11,026), and $ß^+$ (314) are first entered in the appropriate row and column marginal totals. The total in the (OR^+, $ß^+$: 314) cell is the smaller of the two-column totals, $\sum OR^+$ (442) and $\sum ß^+$ (314). Likewise, the total in the (OR^-, $ß^-$: 10,898) cell is the smaller of the two marginal totals, $\sum OR^-$ (10,898) and $\sum ß^-$ (11,026). The totals for remaining two cell totals are determined by subtraction: (OR^+, $ß^-$: 128) = [$\sum OR^+$ (442)] – [OR^+, $ß^+$ (314)] = 128, and (OR^-, $ß^+$: 0): [$\sum OR^-$ (10,898)] - [OR^-, $ß^-$ (10,898)] = 0.

Successive tables in an Excel spreadsheet were coded to compute S^+/S^- and P^+/P^- probabilities in all CMAQ 12 km^2 grids and in grids with and without ambient fine PM air monitors. The Excel tables implemented the computational procedures shown in Fig. 3. The SAS Freq procedure also computes the S^+/S^- probabilities (SAS, 2017; Stokes et al., 2012). A SAS program was written to confirm the accuracy of the Excel spreadsheet computations for the S^+/S^- and P^+/P^- probabilities and statistically evaluate the relationship between the related cells in all the 2 × 2 tables by using the McNemar chi square test (Stokes et al., 2012). The results for the McNemar chi square analyses are included in Tables S1-S3, the last column (supplemental file).

2.11. S^+ probabilities and total observations

The relationships between S^+ probabilities, TP cases, and total observations for the OR case group were evaluated using regression analysis. Proc REG in the SAS/STAT package was used to fit linear functions between total observations, the outcome measure, and S^+ probability, the predictor variable, for the elevated OR case group in all CMAQ 12 km^2 grids, and in grids with monitors and in grids without monitors (SAS, 2018). The linear equation produced by the SAS REG procedure was evaluated for a predetermined range of S^+ probability values in the Excel spreadsheet. The overall purpose of these analyses was to determine the total observations required for each of the four respiratory-cardiovascular chronic disease hospital events (ED asthma, and IP asthma, and MI, and HF hospitalizations) and all four combined in the three grid conditions (all, with and without $PM_{2.5}$ ambient air monitors) to attain a higher S^+ probability of 0.964, than the S^+ probability that was obtained with the study's sample sizes.

3. Results

3.1. Cases and controls

Table 1 includes totals and percentages of cases and controls for each of the four respiratory-cardiovascular chronic disease hospital outcomes, ED visits, and IP hospitalizations, stratified on CMAQ monitor grid status, monitors, and no monitors. By design, there were three case-crossover matched controls for each case. ED asthma had the most observations (47,256), followed by IP HF (27,518), then IP MI (19,201), and IP asthma (13,515) had the fewest observations. For all four health outcomes, there were more observations in CMAQ grids without monitors than in CMAQ grids with monitors, with percentages always greater than 50%: ED asthma, 56%; IP asthma, 58%; IP MI, 63%; and, IP HF, 57%.

3.2. CLR runs, S^+/S^- and P^+/P^- probabilities, and correlations in all grids

CLR results and other statistical analyses for the not-elevated and elevated OR case and not-elevated and elevated ß case groups are included in Table S1 (supplemental file). All CLR ORs for the four health outcomes and five fused surfaces (third column), PMB, and the four experimental AOD-$PM_{2.5}$, were significant, all p's$\leq$0.01. In addition, the elevated OR^+ case group percent (3.1) was significantly higher than the elevated $ß^+$ case group percent (1.6, 95% CI = 1.3–1.9; $p\leq0.05$).

S^+/S^- probabilities for the four health outcomes in all grids are shown in the multi-panel Fig. 4, top row. The first panel, closest to the left margin, displays results for ED asthma.

The second panel from the left margin shows the results for IP asthma. The third panel displays results for IP MI. The last panel, closest to the right margin, shows the results for IP HF. Except for ED asthma's PMB, as seen in the top row, the first panel, which had identical S^+ and S^- probabilities of 1.00, the other three health outcomes had S^- probabilities that were consistently higher than the S^+ probabilities. S^+ probabilities were always higher for the four health outcomes for PMB than the four AOD-$PM_{2.5}$ fused surfaces. For three fused surfaces with CMAQ $PM_{2.5}$ model estimates (A = PMB, D = PMCQ, and E = PMCKQ), S^+ probabilities were consistently higher for PMB, lower for PMCKQ, and intermediate for PMCQ. This pattern suggests that Kriging reduced the PMCKQ S^+ probability more than the PMCQ S^+ probability for the not-Kriged PMCQ fused surface. For PMB and the four AOD-$PM_{2.5}$ fused surfaces, S^- probabilities for ED asthma, IP asthma, and IP HF were equal to 1.00. IP MI had S^- probabilities equivalent to 1.00 for PMB and ~0.87 for the four AOD-$PM_{2.5}$ fused surfaces.

P^+/P^- probabilities in all grids are shown in the multi-panel Fig. 5, top row. The results for the four health outcomes are arranged in the same way as they appeared in Fig. 4 for the S^+/S^- probabilities. ED asthma results are in the first panel closest to the left margin, and the results for IP HF are in the 4th panel, closest to the right margin. Health outcome results for IP asthma and MI are in the 2nd and 3rd panels, from the left margin in the top row. The most salient observation is that P^+ probabilities for all four health outcomes and the four AOD-$PM_{2.5}$ fused surfaces were ~1.00. Except for the ED asthma's PMB fused surface, which had a P^+ probability of 0.97 (please refer to the first panel, top row), the P^+ probabilities for the other three PMBs had values ~1.00. P^- probabilities for the four AOD-$PM_{2.5}$ fused surfaces were ~1.00 for ED asthma, IP asthma, and IP HF. IP MI had P^- probabilities for the four AOD-$PM_{2.5}$ fused surfaces that were at least 0.86, but none attained the maximum value of 1.00. Thus, all four health outcomes had PMB P^- probabilities of 1.00.

Correlations for selected variables in all grids are included in Table S4 (supplemental file). There was a significant correlation between total observations for each of the four health outcome groups and ß% ($p\leq0.01$), with an r^2 = 77.1%. There was also a significant correlation between total observations and S^+ ($p\leq0.01$), with r^2 = 42.8%. There was a significantly negative correlation between ΔOR% and S^+ ($p\leq0.01$), with r^2 = 32.4%. There was a significant correlation between ß% and S^+ ($p\leq0.01$), with r^2 = 54.9%. There were significantly negative correlations between S^+ and S^- ($p\leq0.05$), with r^2 = 20.2%, and between S^+ and P^+ ($p\leq0.05$), with r^2 = 20.2% for each pair of correlations.

3.3. CLR runs, S^+/S^- and P^+/P^- probabilities, and correlations in grids with monitors

Table S2 (supplemental file) includes OR results and the number of elevated and not-elevated observations in the OR case and ß case groups in grids with monitors. All ORs were significant for each of four health outcomes and the five fused surfaces per health outcome (all p's$\leq$0.01). Separate analyses showed that the mean percent for the elevated OR case group (3.0) was significantly higher than the mean percentage for the elevated ß case group (1.0, 95% CI = 1.0–1.1) ($p\leq0.05$).

S^+ and S^- probability analyses for the four health outcomes and the five fused surfaces in grids with monitors are shown in Fig. 4, middle row. All S^+ probabilities were 0.51 or lower, while all S^- probabilities were equal to 1.00. Only ED asthma's PMB (0.46), PMCQ (0.42) fused

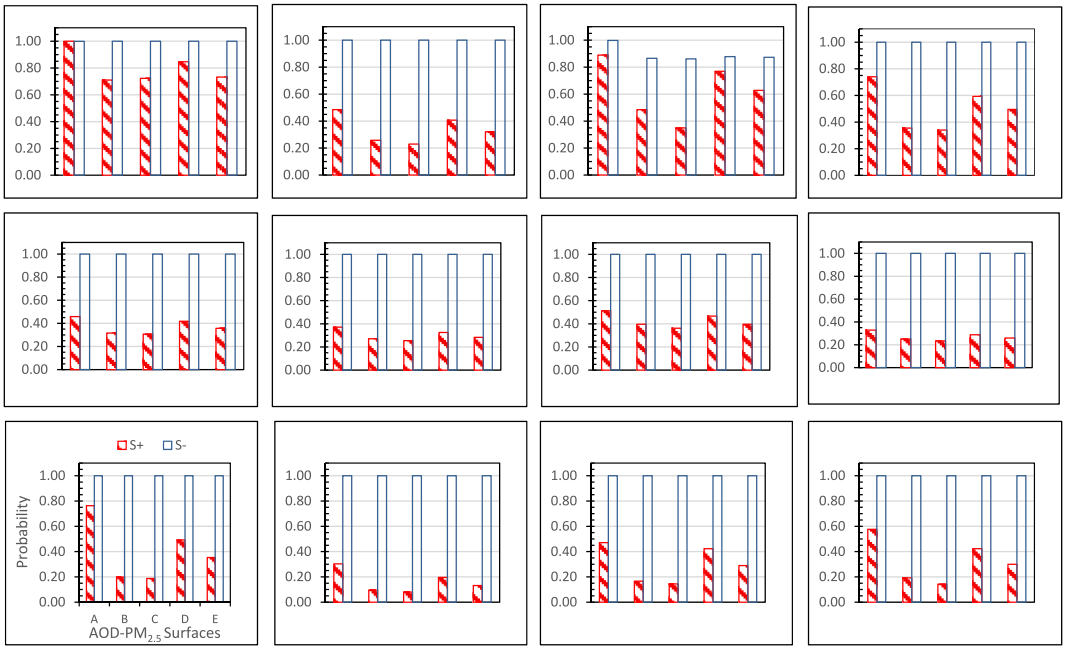

Fig. 4. True positive (TP) cases were identified by using sensitivity (S^+) probabilities and true negative (TN) controls were detected by using specificity (S^-) probabilities for emergency department (ED) asthma visits (1st column) and inpatient (IP) asthma (2nd column), myocardial infarction (MI; 3rd column) and heart failure (HF; 4th column) hospitalizations for the 4 AOD-$PM_{2.5}$ and PMB fused surfaces (A = PMB; B = PMC; C = PMCK; D = PMCQ; and E = PMCKQ) in all CMAQ grids (top row), grids with monitors (middle row) and grids without monitors (bottom row). Higher S probabilities represent either greater accuracy in the identification of persons with the index health outcome (Dx) in the Odds Ratio elevated (OR^+) case group (S^+)/TP cases or greater accuracy in the identification of persons who did not have Dx in the not-elevated OR^- case group (S^-)/TN controls.

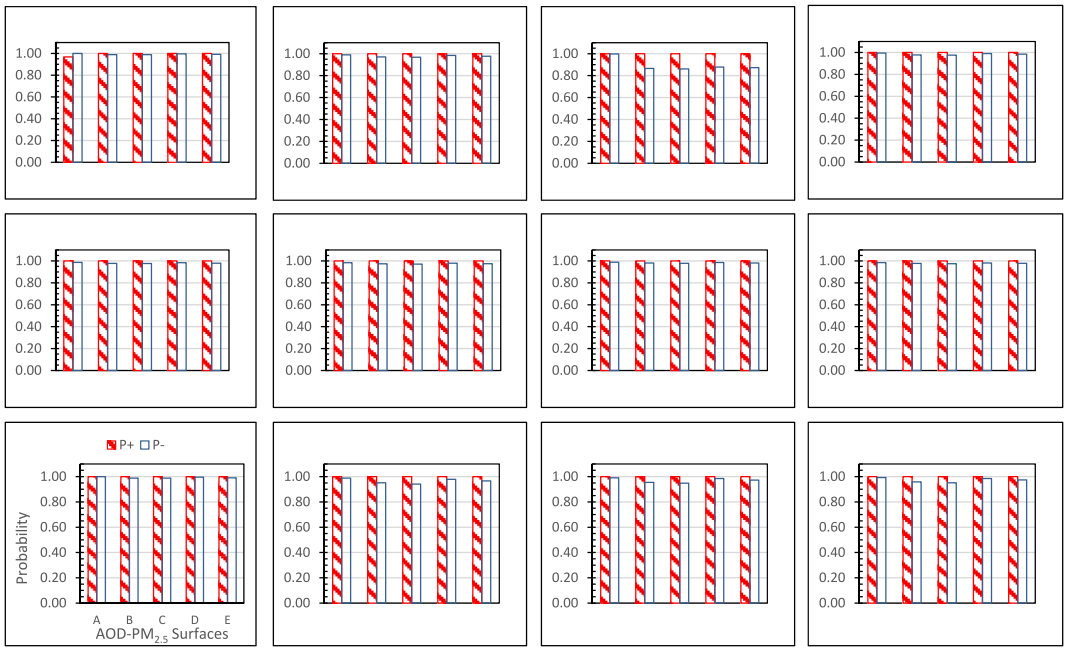

Fig. 5. True positive (TP) cases were identified by using predictive value positive (P^+) probabilities and true negative (TN) controls were determined by using predictive value negative (P^-) probabilities for emergency department (ED) asthma visits (1st column), and inpatient (IP) asthma (2nd column), myocardial infarction (MI) (3rd column) and heart failure (HF) (4th column) hospitalizations for the 4 AOD-$PM_{2.5}$ and PMB fused surfaces (A = PMB; B = PMC; C = PMCK; D = PMCQ; and E = PMCKQ) in all CMAQ grids (top row), grids with monitors (middle row), grids without monitors (bottom row). Higher P probabilities represent either greater accuracy in the correct identification of persons with the index health outcome (Dx) in the elevated Beta ($ß^+$) case group (P^+)/TP cases or greater accuracy in the identification of persons who did not have Dx in the not-elevated Beta ($ß^-$) case group (P^-)/TN controls.

surfaces, and IP MI's PMB (0.51), and PMCQ (0.47) fused surfaces exceeded the low probability threshold of 0.40. Other comparisons between PMB and the four AOD-$PM_{2.5}$ fused surfaces resembled what was previously described above for S^+ probabilities in all CMAQ grids (top row). PMB had the higher S^+ probability values for each of the four health outcomes, followed by PMCQ with intermediate probability values and PMCKQ having the lower probability values. The PMCK fused surface had S^+ probabilities lower than the S^+ probability values for the PMC fused surface.

P^+ and P^- probabilities for the four health outcomes and five fused surfaces in grids with

monitors are displayed in Fig. 5, middle row. All 20 comparisons for the P^+ probabilities and the 20 comparisons for the P^- probabilities had values of ~1.00. Minor differences, nonetheless, were present. All P^+ probability values were equal to 1.00, while all P^- probability values were slightly lower and within the narrow range of 0.97–0.99.

Correlations between total observations, elevated OR case group and ß case group percentages, S^+ and P^- probabilities, in grids with monitors, are included in Table S5 (supplemental file). ΔOR% had significantly negative correlations with S^+ and P^- probabilities (both p's≤0.01); the r^2 values were 31.9% and 82.8%, respectively. ß% was significantly correlated with S^+ (p≤0.01), with r^2 = 64.0%. The correlation between S^+ and P^- was significant (p≤0.01), with r^2 = 71.6%.

3.4. CLR runs, S^+/S^- and P^+/P^- probabilities, and correlations in grids without monitors

Table S3 (supplemental) file shows the CLR runs, percent elevated and total elevated and not-elevated cases in the OR case and ß case groups, in grids without monitors. All 20 CLR runs had significant ORs (all p's≤0.01). The OR case group's percent elevated of 3.9 was significantly higher than the ß case group's percent elevated of 0.9 (95% CI = 0.8–1.1) (p≤0.05).

OR case group's S^+/S^- probabilities for the four health outcomes and the five fused surfaces in CMAQ grids without ambient $PM_{2.5}$ air monitors are shown in Fig. 4, bottom row.

S^+/S^- probabilities in grids without monitors resembled S^+/S^- probabilities for grids with monitors. S^+ probabilities for the four health outcomes and five fused surfaces were lower than the S^- probabilities. The highest S^+ probability occurred for ED asthma's PMB fused surface (0.76). The four health outcomes showed the same S^+ probability relationship for the three fused surfaces that included the CMAQ $PM_{2.5}$ model estimates: S^+ probability was consistently higher for PMB, intermediate for PMCQ, and lower for PMCKQ. Another robust outcome among the four AOD-$PM_{2.5}$ fused surfaces was that while PMC resembled PMCK, they both had S^+ probabilities that were consistently lower than the PMCQ and PMCKQ S^+ probabilities. All 20 S^- probability values were equal to 1.00.

ß case group P^+/P^- probabilities for the four health outcomes, PMB and the four AOD-$PM_{2.5}$ fused surfaces, in grids without air monitors are shown in Fig. 5, bottom row. The

most prominent finding was that all 20 P^+ probability values were 1.00, and the 20 P^- probability values were ~1.00. There were minor differences, however, among the P^- probability values for the four health outcomes. For example, the five P^- probability values for ED asthma were equal to 0.99 or 1.00. The P^- probability values were slightly lower for the other three health outcomes, with minimum-maximum values of 0.94–0.99.

Correlation analyses are included in Table S6 (supplemental file). The total observations variable was significantly associated with ß% (p≤0.01), r^2 = 72.1%. ΔOR% had a near-perfect inverse correlation with P^- (p≤0.01) and a high r^2 value of 94.9%.

3.5. Grids with and without monitors

Additional analyses were completed to determine if the correct identification of TP cases and TN controls differed in CMAQ grids with and without monitors. Secondary analyses evaluated results in all grids and grids with or without monitors. These analyses were included in Tables S7-S15 (supplemental file). More critical findings will be briefly

summarized below.

3.5.1. ΔOR% and ß% (Table S7)

While ΔOR% was significantly higher in grids without monitors (3.9) than in grids with monitors (3.0, 95% CI = 2.8–3.2) ($p \leq 0.05$), the ß% was significantly lower in grids without monitors (0.9) than in grids with monitors (1.0, 1.0–1.1), and in all grids (1.6, 1.3–1.9) (both p's$\leq$0.05).

3.5.2. ΔOR% and ß%: AOD $PM_{2.5}$ fused surfaces (Table S8)

Only OR case group comparisons had significantly higher ΔOR% values in grids without monitors than in grids with monitors for three AOD-$PM_{2.5}$ fused surfaces: PMC (5.3; 3.2, 95% CI = 2.8–3.7), PMCK (6.0; 3.4, 95% CI = 3.1–3.8) and PMCKQ (3.8; 3.2, 95% CI = 2.8–3.5) (all p's$\leq$0.05). In a reversal to this trend, the PMB fused surface had significantly lower ΔOR% values in grids without monitors (1.7) compared to grids with monitors (2.4, 95% CI = 2.2–2.7), and in all grids (2.0, 95% CI = 1.8–2.1), both p's$\leq$0.05. All ß case group comparisons were not significantly different between grids without and with air monitors (all p's$>$0.05).

3.5.3. ΔOR% and ß%: Health outcomes (Table S9)

For all four health outcomes, the OR case group had significantly higher ΔOR% values in grids without monitors compared to grids with monitors: ED asthma (3.9; 3.0, 95% CI = 2.6–3.5), IP asthma (4.0; 3.3, 95% CI = 2.7–3.9), IP MI (3.9; 2.9, 95% CI = 2.4–3.4), and IP HF (3.7; 2.8, 95% CI = 2.4–3.2) (all p's$\leq$0.05). The ß case group did not have significantly different ß% values in grids without and in grids with air monitors (all p's$>$0.05).

3.6. S^+/S^- and P^+/P^- (Table S10)

S^+ probabilities for the OR case group were significantly lower in grids without monitors (0.30) than in grids with monitors (0.34, 95% CI = 0.31–0.38) and in all grids (0.57, 95% CI = 0.46–0.67) (both p's$\leq$0.05). The OR case group $\Delta(S^- - S^+)$ value was significantly higher in grids without monitors (0.70) than in grids with monitors (0.66, 95% CI = 0.62–0.69), and in all grids (0.43, 95% CI = 0.33–0.54) (both p's$\leq$0.05). P^- probabilities for the ß case group were significantly lower in grids without monitors (0.97) than in grids with monitors (0.98, 95% CI = 0.98–0.98) ($p \leq 0.05$).

3.6.1. S^+/S^- and P^+/P^-: AOD $PM_{2.5}$ fused surfaces (Tables S11 and S12, respectively)

As shown in Table S11, OR case group S^+ probabilities were significantly lower in grids without monitors than in grids with monitors for PMC (0.17; 0.31, 95% CI = 0.21–0.41) and PMCK (0.14; 0.29, 95% CI = 0.20–0.38) (both p's$\leq$0.05). OR case group $\Delta(S^- - S^+)$ values were significantly higher in grids without monitors than in grids with monitors for PMC (0.84; 0.69, 95% CI = 0.59–0.79) and PMCK (0.86; 0.71, 95% CI = 0.62–0.80) (both p's$\leq$0.05).

Table S12 shows that the ß case group P^- values were significantly lower in grids without monitors than in grids with monitors for PMC (0.96; 0.98, 95% CI = 0.97–0.98) and PMCK (0.95; 0.98, 95% CI = 0.97–0.98) (both p's$\leq$0.05).

3.6.2. S^+/S^- and P^+/P^-: Health outcomes (Tables S13 and S14, respectively)

Results presented in Table S13 show that OR case group S^+ probabilities were significantly higher in grids without monitors than in grids with monitors for IP HF (0.33; 0.27, 95% CI = 0.23–0.32), and significantly lower in grids without monitors than in grids with monitors for IP asthma (0.16; 0.30, 95% CI = 0.24–0.36) and IP MI (0.30; 0.43, 95% CI = 0.45–0.50) (all p's$\leq$0.05).

As displayed in Table S14, the ß case group P^- probability values were significantly lower in grids without monitors than in grids with monitors only for IP MI (0.97; 0.98, 95% CI = 0.98–0.99) ($p \leq 0.05$).

3.7. OR-case group S^+ probabilities and total observations (Table S15)

Regression analyses estimated the number of health outcome observations that would be required to increase the OR case group's S^+ probability value to 0.964. Regression results are summarized in Table S15. Only the regression runs for the Both, and No monitor grid conditions had significant predictor (sensitivity) outcomes, $p \leq 0.05$. For Both monitor grid conditions, 10,073 cases per health outcome group would be needed to attain an S^+ probability of 0.964. In grids without monitors, 6,710 observations per health outcome group would be required to arrive at an S^+ probability of 0.964.

For all four health outcome groups, ED asthma, IP asthma, MI, and HF hospitalizations, 10,073 per health outcome group x 4 health outcome groups = 40,292 cases needed to attain the S^+ probability of 0.964. This outcome is a 50.8% increase from the total cases that were available in this data analysis study, as shown in Table 1: ED Asthma (11,723), IP Asthma (3,376), IP MI (4,790), and IP HF (6,826) – combined total observations of 26,715. For three of the four chronic disease hospital outcome groups, it would require increases of 198.4% for IP asthma (from 3,376), 110.3% for IP MI (from 4,790), and 47.6% for IP HF (from 6,826). The study's ED asthma case sample size of 11,723 exceeded the required ED asthma case sample size of 10,073.

Regression results for the No monitor grid group determined that 6,710 total health outcome cases would be required for each health outcome group to attain an OR case group S^+ probability of 0.964. The four health outcomes combined resulted in a total of 15,434 observations: ED Asthma contributing 6,571; IP Asthma, 1,959; IP MI, 3,006; IP HF, 3,898. Total observations for all four health outcomes combined in the No monitor group would have to be increased by 73.9% to attain the OR case group S^+ probability of 0.964. For each of the four No monitor group health outcomes, it would mean that the ED asthma cases would have to be increased 2.1% (from 6,571), 242.5% for IP asthma (1,959), 123.2% for IP MI (3,006), and 72.1% for IP HF (3,898).

4. Discussion

To our knowledge, this is the first environmental epidemiology air pollution study to complete an analysis of TP cases and TN controls for respiratory-cardiovascular chronic disease ED visits and IP hospitalizations in a case-crossover analysis of AOD-$PM_{2.5}$ concentration levels in urban (with air monitors) and rural (without air monitors) areas. Study results demonstrated that both valid and reliable identification of TP cases and TN controls for four respiratory-cardiovascular chronic diseases were possible for the ß case group in all CMAQ monitor grids and grids with and without air monitors. However, only TN controls, not TP cases, could be reliably and accurately estimated with S^- probabilities ~1.00 in all CMAQ grid conditions for the OR case group. Furthermore, unlike the ß case group, the OR case group S^+ probabilities depended on the number of available cases in the input files. Regression analyses

Table 1
Total (percent) of cases and controls in all CMAQ grids and in grids with and without ambient $PM_{2.5}$ air monitors included in four respiratory-cardiovascular chronic disease health outcomes.

outcome	cases	controls	total
ED Asthma	11,723 (24.81)	35,533 (75.19)	47,256 (100.00)
Monitor	5,152 (10.90)	15,663 (33.14)	20,815 (44.05)
No Monitor	6,571 (13.91)	19,870 (42.05)	26,441 (55.95)
IP Asthma	3,376 (24.98)	10,139 (75.02)	13,515 (100.00)
Monitor	1,417 (10.48)	4,255 (31.48)	5,672 (41.97)
No Monitor	1,959 (14.50)	5,884 (43.54)	7,843 (58.03)
IP MI	4,790 (24.95)	14,411 (75.05)	19,201 (100.00)
Monitor	1,784 (9.29)	5,401 (28.13)	7,185 (37.42)
No Monitor	3,006 (15.66)	9,010 (46.92)	12,016 (62.58)
IP HF	6,826 (24.81)	20,692 (75.19)	27,518 (100.00)
Monitor	2,928 (10.64)	8,906 (32.36)	11,834 (43.00)
No Monitor	3,898 (14.17)	11,786 (42.83)	15,684 (57.00)

demonstrated that OR case group S^+ probabilities of 0.964 in all CMAQ grids could be attained, provided that total available cases for IP asthma, IP MI, and IP HF were increased by 198.4%, 110.3%, and 47.6%, respectively. Another new and important finding was confirmation that the OR case group significantly overestimated the number and percentage of TP ED asthma visits, IP asthma, MI, and HF hospitalization cases, relative to the TP cases estimates produced by the ß case group.

This new information about the reliability and validity of respiratory-cardiovascular TP cases and TN controls has essential consequences for completing similar studies in the US and other countries (Hennekens and Buring, 1987; Kelsey et al., 1996; Last, 1995; Schlesselman, 1982). Of importance, these results suggest that it is not possible to use the OR case group algorithm to accurately estimate the occurrence of TP cases in a case-crossover formatted AOD-$PM_{2.5}$ and health outcome file. For each of the four chronic disease ED visits and IP hospitalizations included in this study, OR-based percentages for TP cases were significantly higher than the ß-based percentages for TP cases in all grid conditions.

One parsimonious explanation could be that the total number of cases in the elevated OR case group was smaller than the total number of controls in the not-elevated OR case group, by at least one order of magnitude, from about one hundred to one thousand. As a result, fewer FP cases are required to lower the S^+ probability by a constant of 0.10 than would be necessary to decrease the S^- probability value for the same constant, 0.10. One obvious solution would be to increase the number of cases and the number of matched controls. The newly developed and evaluated ß case group algorithm is more accurate than the OR case group algorithm in determining the percentage of TP cases since this algorithm is based on the evaluation of cases and controls in each stratum, where the case's ß value is significantly higher than the mean ß value for the three matched controls. When both methods are available to estimate the number and percentage of TP cases, the ß case group estimate should be selected. The OR case group algorithm should be used to estimate the number and percentage of TP cases only when it is not possible to implement the ß case group algorithm.

For S^- and P^+/P^- probabilities, there were no apparent differences between urban and rural CMAQ 12 km^2 grids regarding TP cases (P^+) and TN controls (P^-, S^-). This study's finding is essential for using health outcome measures to evaluate the strength of the association between elevated AOD-$PM_{2.5}$ concentration levels in grids with and without ambient $PM_{2.5}$ air monitors. In addition, because of the established statistical association between on-the-ground $PM_{2.5}$ monitor measurements and satellite AOD unitless readings, it is possible to use AOD-$PM_{2.5}$ concentration level readings as proxies for actual ambient $PM_{2.5}$ concentration level measurements in urban areas. However, these AOD-$PM_{2.5}$ statistical validation studies have been completed only in urban areas where $PM_{2.5}$ monitors have been placed. Thus far, it has not been possible to undertake a similar AOD-$PM_{2.5}$ reliability and validity study in rural areas because there are no on-the-ground air monitors (Fu et al., 2020; Han et al., 2020; Lee et al., 2016a, 2016b; Prud'homme et al., 2013; Sorek-Hamer et al., 2016).

Probability measurements represent the accuracy with which the two algorithms can reliably detect chronic disease TP cases and TN controls, one for the OR case group and the other for the newly developed ß case group. Higher probabilities represent a higher degree of accuracy with which an algorithm can detect TP cases and TN controls. The S^- and P^- probabilities were ~1.00 for TN controls. Only the P^+ was ~1.00 for TP cases.

For these three probability measures of P^+/P^- and S^-, there were no apparent differences between grids with and without air monitors. The unique contribution of this data analysis study is that it evaluated four different AOD-$PM_{2.5}$ fused surfaces and four different respiratory-cardiovascular hospital events. Study results found no differences between grids with and without air monitors for each of the 16 separate AOD-$PM_{2.5}$ and health outcome analyses. Similar results were obtained for the association between PMB and ED asthma, IP asthma, IP MI, and IP HF. These results, then, provide indirect confirmation, for the first time, that the concentration-response function that describes the relationship between AOD-$PM_{2.5}$ and respiratory-cardiovascular ED visits and IP hospitalizations remained unchanged (i.e., no significant differences) in grids with and in grids without air monitor.

Reliability and validity assessment of TP cases and TN controls requires the section of a cutoff point. In the implementation of the ß case group algorithm, the Z value of 1.645 was selected because it has a p=0.05, one-tail. Published scientific studies in epidemiologic specialty areas continue to use p=0.05 to identify rare events (Agresti, 2002; Armitage et al., 2002; Hennekens and Buring, 1987; Hosmer et al., 2013; Kelsey et al., 1996; Schlesselman, 1982; Stokes et al., 2012). Selecting a Z value with a two-tail p=0.05 would have resulted in the identification of fewer TP cases, thereby making the difference in the number and percentage of TP cases identified by the OR case group and the ß case group even more extreme. The only other option would have been to select another Z cutoff point besides 1.645. This latter option would have required a parametric analysis of a range of Z values and the number and percentage of TP cases and TN controls that would have occurred. This last option was not undertaken because this analysis was not within the two objectives of this study.

Different methodological strengths support the soundness of these study results. The first contribution was using four other experimental AOD-$PM_{2.5}$ fused surfaces and four different health outcomes in grids with and without air monitors, thereby making the study's results generalizable. The second strength was developing and evaluating the new ß case group algorithm to detect TP cases and TN controls reliably and validly and comparing these results to the outcomes from the OR case group algorithm. The four probability values, two each for the ß (P^+/P^-) and OR (S^+/S^-) case groups, provided a novel way to quantify the reliability of detecting TP cases and TN controls. The third contribution was the confirmation that both the ß case group (P^-) and OR case group (S^-) algorithms demonstrated near-perfect agreement, with computed probability values ~1.00, in the detection of TN controls, in all three grid conditions. The fourth contribution confirmed that lower probabilities occurred for the OR case group (S^+) because this algorithm is more sensitive to sample size than the ß case group algorithm. The fifth strength demonstrated that the OR case group's S^+ probabilities could be increased to values ~1.00 by increasing the number of available cases (and matched controls) in the input data files for the four health outcomes. The remaining but essential contribution of this study was the demonstration, for the first time, that there were no differences in the occurrence of TP cases and TN controls in grids with and without air monitors. This last outcome provides indirect evidence that the relationship between AOD-$PM_{2.5}$ concentration levels and the occurrence of respiratory-cardiovascular ED visits and IP hospitalizations in grids with and without air monitors remains unchanged. A related conclusion could be stated, with caution, that the AOD-$PM_{2.5}$ concentration levels documented in grids with air monitors should have the same (or similar) relationship to health outcomes in grids without air monitors.

A methodological limitation of this study, however, concerns the complete reliance on ED visits and IP hospitalizations that were only available in electronic files, without further opportunities to access the underlying patient medical records, from which the electronic hospital event information was abstracted (Cozzolino et al., 2019; Rosamond et al., 2004). Thus, it is possible that an unknown number and proportion of asthma, MI, and HF patient diagnoses could also include FP respiratory-cardiovascular cases (controls; Cozzolino et al., 2019; Rosamond et al., 2004).

Cozzolino et al. (2019) reported high S^+/S^-, P^+/P^- and TP/TN probabilities for MI (total medical charts, 128; 91%–98%) and HF (medical charts, 127; 90%–96%). They concluded that these Umbria (Perugia, Italy) healthcare administrative databases can be used in epidemiologic studies. Rosamond and associates (2004) evaluated differences in S^+, P^+ and FP probabilities between inclusion criteria in four

US communities in the different US States (North Carolina, Mississippi, Minnesota, and Maryland) and reviewed medical charts that included ICD-9-CM MI hospital discharge diagnoses. S^+ probabilities were higher for: males (0.65) than females (0.60); Whites (0.67) than Blacks (0.61); and, higher in Maryland (0.77) and Minnesota (0.71) than in North Carolina (0.57) and Mississippi (0.56). P^+ were also higher for males (0.77), Whites (0.76), and North Carolina (0.78). FP probabilities were lower for females (0.03), equivalent for ethnicity (0.03), and lower in North Carolina and Mississippi (0.03) than in Minnesota and Maryland (0.04). Gender and ethnic differences remained between 1987 and 2000. The study authors suggested investing additional resources in validation work to be completed by ongoing surveillance projects.

The findings from the Cozzolino et al. (2019) and Rosamond and associates (2004) studies have implications for the unconfirmed accuracy for MI and HF diagnoses included in the Maryland HSCRC electronic IP records. For example, the ED asthma or IP asthma cases entered in the Maryland HSCRC electronic hospital files, ambulatory and inpatient, and included in this data analysis study, may not have been correctly diagnosed as asthma patients. The incorrect diagnosis of asthma represents the occurrence of FP asthma cases (control). FP cases could have occurred not only for asthma but also MI and HF. Another methodological limitation concerns the possibility of incorrect recording of the patient's residential information, coded as the ZIP code of residence, in the medical chart. Still, another limitation could have occurred as the patient's information recorded in the medical chart was computer entered into the electronic reporting system established by the Maryland HSCRC. To summarize, it is possible that not all ICD-9-CM codes and residential ZIP codes were accurately transmitted to the Maryland HSCRC.

From the available information on the Maryland HSCRC website in 2020, the percentage of incorrectly entered ICD-9-CM codes and residential ZIP codes should not be a major issue for the electronic IP and ambulatory (ED) files (HSCRC, 2020) because of implemented data quality control checks. Similar data quality protocols were also implemented for the processing of the 2004–2006 electronic patient records.

In the most recent guidance to Maryland hospitals, the Maryland HSCRC stated, on its website, in 2020, that data entry errors for a predetermined group of variables in the IP and ED electronic records *cannot* exceed 10% in each electronic patient record file (HSCRC, 2020). Starting in 2021, the tolerated 10% error rate will be reduced to 5% for each electronic record file (HSCRC, 2020). In addition, the medical recorded number, date of admission, date of discharge variables in the IP electronic file, and the medical record number and from-through service dates in the ED electronic file were evaluated and found to be 100% complete (HSCRC, 2020).

The fact that P^+/P^- probabilities for the ß case group and the S^- probabilities for the OR case group could also reliably and validly identify elevated (TP cases) and not-elevated (TN controls) cases in grids with and without ambient $PM_{2.5}$ air monitors suggests that the experimental AOD-$PM_{2.5}$ fused surfaces developed by our research group can be utilized in 12 km^2 CMAQ grids with and without ambient fine PM air monitors to evaluate the association between elevated ambient fine PM levels and respiratory-cardiovascular chronic disease ED visits and IP hospitalizations in urban and in rural areas. Since ambient $PM_{2.5}$ monitors are usually found in urban areas with higher population density and lower economic resources (higher poverty) among residents, published studies have already provided a robust baseline of results that document the detrimental effects of high ambient fine and coarse PM concentration levels on respiratory-cardiovascular chronic disease ED visits and IP hospitalizations (Bell and Ebisu, 2012; Braggio et al., 2020; Brochu et al., 2011; Brook et al., 2010, 2014, 2015; Egondi et al., 2018). Unfortunately, the currently available published literature includes *fewer* studies documenting how elevated ambient fine PM levels increase ED asthma visits, IP asthma, MI, and HF hospitalizations in rural areas. The results from this study suggest, for the first time, that the use of AOD-$PM_{2.5}$ fused surfaces and respiratory-cardiovascular hospital events in rural areas, where ambient fine PM air monitors may not be available in the US, may make it possible to identify TP cases and TN controls correctly. The recent Braggio and associates (2020) publication and findings from this study suggest that it may be possible to use PMC and PMCK fused surfaces in urban and rural areas as proxies for elevated ambient $PM_{2.5}$ concentration levels in epidemiologic studies. Among these two experimental AOD-$PM_{2.5}$ fused surfaces, the use of PMCK may be more appropriate than the use of PMC because the former fused surface does not have missing readings. Which AOD-$PM_{2.5}$ fused surface is selected should be determined by considering the study's purpose and related methodologic considerations.

5. Conclusion

Study results confirmed that the currently available OR case group algorithm significantly overestimated the percentage of TP cases and had lower and less reliable probabilities for identifying TP cases. The OR case algorithm was only able to reliably and validly identify TN controls. The ß case group algorithm reliably and validly identified TP cases and TN controls in all three grid conditions. Therefore, when both algorithms can be computed, the first consideration should be given to the use of the ß case group algorithm. Because the number and percentage of TP cases and TN controls did not differ between grids with and grids without monitors, these epidemiologic results suggest for the first time that the concentration-response function that describes the relationship between AOD-$PM_{2.5}$ and respiratory-cardiovascular health outcomes *may be similar* in grids with (urban) and grids without (rural) air monitors, but *only* in states that resemble Maryland in its smaller land area, in urban grids with 17 ambient air monitors in 2004-2006 and smaller rural areas without ambient air monitors. In conclusion, future epidemiologic investigations utilizing respiratory-cardiovascular hospital events in rural areas should consider selecting the most appropriate AOD-$PM_{2.5}$ fused surface, PMC or PMCK, as a way of estimating ambient $PM_{2.5}$ concentration levels.

Funding

A National Aeronautics and Space Administration Grant (NNH11CD19C) funded this research for Earth Science Applications Feasibility Studies: Public Health, awarded to the Battelle Memorial Institute, Columbus, Ohio.

CRediT authorship contribution statement

John T. Braggio: Conceptualization, Data curation, Formal analysis, Funding acquisition, Investigation, Methodology, Supervision, Validation, Visualization, Writing – original draft, Writing – review & editingwriting, review, and editing. **Eric S. Hall:** Conceptualization, Methodology, Project administration, Resources, Software, Validation, Writing – review & editingwriting, review, and editing. **Stephanie A. Weber:** Methodology, Validation, Writing – review & editing, Funding acquisition. **Amy K. Huff:** Funding acquisition, Methodology, Validation, Formal analysis, Writing – review & editingwriting, review, and editing, All authors have read and agreed to the published version of the manuscript.

Declaration of competing interest

The authors declare that they have no known competing financial interests or personal relationships that could have appeared to influence the work reported in this paper.

Acknowledgments

Fred Dimmick, EPA, facilitated inter-agency collaboration on this data linkage and analysis project, and two prior CDC-EPA data linkage

studies; Eric S. Hall, EPA, continued inter-agency collaboration between CDC-EPA on this data linkage and analysis project and was the co-developer of the HBM used in the analyses; Michelle Morara, Battelle Memorial Institute, HBM update, from two to three input surfaces (with or without missing observations). Judy Qualters, CDC, endorsement, and support of this data linkage and analysis project.

Appendix A. Supplementary data

Supplementary data to this article can be found online at https://doi.org/10.1016/j.atmosenv.2021.118629.

Disclaimer

EPA, through its Office of Research and Development, participated in this data analysis project. This manuscript went through Agency review, and it was approved for publication. Although this work was reviewed by the EPA and approved for publication, it may not necessarily reflect the official Agency policy. Mention of trade names or commercial products in this manuscript does not constitute endorsement or recommendation for use by the EPA or the authors.

References

Agresti, A., 2002. Categorical Data Analysis, second ed. John Wiley & Sons, Inc., Hoboken, New Jersey, ISBN 0-471-36093-7.

Altman, D.G., Bland, J.M., 1994a. Diagnostic tests 1: sensitivity and specificity. BMJ 308, 1552. https://doi.org/10.1136/bmj.308.6943.1552.

Altman, D.G., Bland, J.M., 1994b. Diagnostic tests 2: predictive values. BMJ 309, 102. https://doi.org/10.1136/bmj.309.6947.102.

Amsalu, E., Wang, T., Li, H., Liu, Y., Wang, A., Liu, X., et al., 2019. Acute effects of fine particulate matter ($PM_{2.5}$) on hospital admissions for cardiovascular disease in Beijing, China: a time-series study. Environ. Health 18, 70. https://doi.org/10.1186/s12940-019-0506-2.

Argacha, J.F., Collart, P., Wauters, A., Kayaert, P., Lochy, S., Schoors, D., et al., 2016. Air pollution and ST-elevation myocardial infarction: a case-crossover study of the Belgian STEMI Registry 2009-2013. Int. J. Cardiol. 233, P300–P305. https://doi.org/10.1016/J.IJCARD.2016.07.191.

Armitage, P., Berry, G., Matthews, J.N.S., 2002. Statistical Methods in Medical Research, fourth ed. Blackwell Science, Inc., Malden, Massachusetts, ISBN 0-632-05257-0.

Babin, S., Burkom, H., Holtry, R., Tabernero, N., Davies-Cole, J., Stokes, L., et al., 2008. Medicaid patient asthma-related acute care visits and their associations with ozone and particulates in Washington, DC, from 1994-2005. Int. J. Environ. Health Res. 18, 209–221. https://doi.org/10.1080/09603120701694091.

Bell, M.L., Ebisu, K., 2012. Environmental inequality in exposures to airborne particulate matter components in the United States. Environ. Health Perspect. 120, 1699–1704. https://doi.org/10.1289/ehp.1205201.

Belle, J.H., Liu, Y., 2016. Evaluation of Aqua MODIS Collection 6 AOD parameters for air quality research over the Continental United States. Rem. Sens. 8, 815. https://doi.org/10.3390/rs8100815.

Braggio T., J., Brunner, W., Lutzker, L., Managan, A., Simms, E., Tomasallo, C., et al., 2012. Analysis of 2009 Pollen Readings in Atlanta, GA. Poster presented at the Council of State and Territorial Epidemiologists Annual Conference, Omaha, NE, June 3-7, 2012, Baltimore, MD, and Madison, WI. Available online at: https://cdn.ymaws.com/www.cste.org/resource/resmgr/EnvironmentalHealth/AYipPollenAtlantaBaltimoreMa.pdf. (Accessed 30 September 2020).

Braggio, J.T., Hall, E.S., Weber, S.A., Huff, A.K., 2020. Contribution of satellite-derived aerosol optical depth $PM_{2.5}$ Bayesian concentration surfaces to respiratory-cardiovascular chronic disease hospitalizations in Baltimore, Maryland. Atmosphere 11, 209. https://doi.org/10.3390/atmos11020209.

Braggio, J.T., Weber, S., Young, E., Hall, E., 2014. Contribution of Hierarchical Bayesian and Aerosol Optical Depth $PM_{2.5}$ Sources to Respiratory-Cardiovascular Chronic Diseases. Presented at the International Society for Environmental Epidemiology Conference, Seattle, WA. August 24-28, 2014. Available online at: https://ehp.niehs.nih.gov/doi/10.1289/isee.2014.P1-149. (Accessed 30 September 2020).

Brochu, P.J., Yanosky, J.D., Paciorek, C.J., Schwartz, J., Chen, J.T., Herrick, R.F., et al., 2011. Particulate air pollution and socioeconomic position in rural and urban areas of the Northeastern United States. Am. J. Publ. Health 101, S224–S230. https://doi.org/10.2015/AJPH.2011.300232.

Brook, R.D., Bard, R.L., Morishita, M., Dvonch, J.T., Wang, L., Yang, H.Y., et al., 2014. Hemodynamic, autonomic, and vascular effects of exposure to coarse particulate matter air pollution from a rural location. Environ. Health Perspect. 122, 624–630. https://doi.org/10.1289/ehp.1306595.

Brook, R.D., Kousha, T., 2015. Air pollution and emergency department visit for hypertension in Edmonton and Calgary, Canada: a case-crossover study. Am. J. Hypertens. 28, 1121–1126. https://doi.org/10.1093/ajh/hpu302.

Brook, R.D., Rajagopalan, S., Pope III, A., Brook, J.R., Bhatnagar, A., Diez-Roux, A.V., et al., 2010. Particulate matter air pollution and cardiovascular disease: an update to the scientific statement from the American Heart Association. Circulation 121, 2331–2378. https://doi.org/10.1161/CIR.0b013e3181dbece1.

Carracedo-Martínez, E., Taracido, M., Tobias, A., Saez, M., Figueiras, A., 2010. Case-crossover analysis of air pollution health effects: a systematic review of methodology and application. Environ. Health Perspect. 118, 1173–1182. https://doi.org/10.1289/ehp.0901485.

CDC (U.S. Centers for Disease Control and Prevention), 2020. International Classification of Diseases, Ninth Revision, Clinical Modification (ICD-9-CM). Available online at: https://www.cdc.gov/nchs/icd/icd9cm.htm. (Accessed 30 September 2020).

Chang, H.H., Hu, X., Liu, Y., 2014. Calibrating MODIS aerosol optical depth for predicting daily $PM_{2.5}$ concentrations via statistical downscaling. J. Expo. Sci. Environ. Epidemiol. 24, 398–404. https://doi.org/10.1038/jes.2013.90.

Chen, K., Glonek, G., Hansen, A., Williams, S., Tuke, J., Salter, A., et al., 2016. The effects of air pollution on asthma hospital admissions in Adelaide, South Australia, 2003-2013: time-series and case-crossover analyses. Clin. Exp. Allergy 46, 1416–1430. https://doi.org/10.1111/cea.12795.

Cheng, M.H., Chen, C.C., Chiu, H.F., Yang, C.Y., 2014. Fine particulate air pollution and hospital admissions for asthma: a case-crossover study in Taipei. J. Toxicol. Environ. Health 77, 1075–1083. https://doi.org/10.1080/15287394.2014.922387.

Christopher, S., Gupta, P., 2020. Global distribution of column satellite aerosol optical depth to surface $PM_{2.5}$ relationships. Rem. Sens. 12, 1985. https://doi.org/10.3390/rs12121985.

Chu, Y., Liu, Y., Li, X., Liu, Z., Lu, H., Lu, Y., et al., 2016. A Review on predicting ground $PM_{2.5}$ concentration using satellite aerosol optical depth. Atmosphere 7, 129. https://doi.org/10.3390/atmos7100129.

Cordova, J.E.D., Aguirre, V.T., Apestegui, V.V., Ibarguen, L.O., Vu, B.N., Steenland, K., et al., 2020. Association of $PM_{2.5}$ concentration with health center outpatient visits for respiratory diseases of children under 5 years old in Lima, Peru. Environ. Health 19, 7. https://doi.org/10.1186/s12940-020-0564-5.

Cozzolino, F., Montedori, A., Abraha, I., Eusebi, P., Grisci, C., Heymann, A.J., et al., 2019. A diagnostic accuracy study validating cardiovascular ICD-9-CM codes in healthcare administrative databases. The Umbria data-value project. PloS One 14, e0218919. https://doi.org/10.1371/journal.pone.0218919.

Dai, X., Liu, H., Chen, D., Zhang, J., 2018. Association between ambient particulate matter concentrations and hospitalization for ischemic heart diseases (I20-I25, ICD-10) in China: a multicity case-crossover study. Atmos. Environ. 186, 129–135. https://doi.org/10.1016/j.atmosenv.2018.05.033.

Di, Q., Amini, H., Shi, L., Kloog, I., Silvern, R., Kelly, J., et al., 2019. An ensemble-based model of $PM_{2.5}$ concentration across the contiguous United Stated with high spatiotemporal resolution. Environ. Int. 130, 104909 https://doi.org/10.1016/j.envint.2019.104909.

Egondi, T., Ettarh, R., Kyobutungi, C., Ng, N., Rocklöv, J., 2018. Exposure to outdoor particles ($PM_{2.5}$) and associated child morbidity and mortality in socially deprived neighborhoods of Nairobi, Kenya. Atmosphere 9, 351. https://doi.org/10.3390/atmos9090351.

Engel-Cox, J.A., Holloman, C.H., Coutant, B.W., Hoff, R.M., 2004. Qualitative and quantitative evaluation of MODIS satellite sensor data for regional and urban scale quality. Atmos. Environ. 38, 2495–2509. https://doi.org/10.1016/j.atmosenv.2004.01.039.

EPA US (Environmental Protection Agency), 2020a. Air Quality System (AQS). Available Online at: https://www.epa.gov/aqs. (Accessed 30 September 2020).

EPA US (Environmental Protection Agency), 2020b. Community Modeling and Analysis System (CMAS), CMAQ. Available online at: https://www.cmascenter.org/. (Accessed 30 September 2020).

ESRI (Environmental Systems Research Institute), 2020. ArcGIS Desktop (ArcMap), Release 10.8. Environmental Systems Research Institute, Redlands, CA, USA.

Foley, K.M., Roselle, S.J., Appel, K.W., Bhave, P.V., Pleim, J.E., Otte, T.L., et al., 2010. Incremental testing of the Community Multiscale Air Quality (CMAQ) modeling system version 4.7. Geosci. Model Dev. (GMD) 3, 205–226. www.geosci-model-dev.net/3/205/2010/.

Fu, D., Song, Z., Zhang, X., Wu, Y., Duan, M., Pu, W., et al., 2020. Similarities and differences in the temporal variability of $PM_{2.5}$ and AOD between urban and rural stations in Beijing. Rem. Sens. 12, 1193. https://doi.org/10.3390/rs12071193.

Garcia, E., Berhane, K.T., Islam, T., McConnell, R., Urman, R., Chen, Z., et al., 2019. Association of changes in air quality with incident asthma in children in California. J. Am. Med. Assoc. 321, 1906–1915. https://doi.org/10.1001/jama.219.5357, 1993-2014.

Gehring, U., Wijga, A.H., Hoek, G., Bellander, T., Berdel, D., Brüske, I., et al., 2015. Exposure to air pollution and development of asthma and rhinoconjunctivitis throughout childhood and adolescence: *a* population-based birth cohort study. Lancet Respir. Med. 3, P933–P942. https://doi.org/10.1016/S2213-2600(15)00426-9.

Geng, G., Murray, N.L., Chang, H.H., Liu, Y., 2018. The sensitivity of satellite-based $PM_{2.5}$ estimates to its inputs: implications to model development in data-poor regions. Environ. Int. 121, 550–560. https://doi.org/10.1016/j.envint.2018.09.051.

German, R.R., 2000. Sensitivity and predictive value positive measurements for public health surveillance systems. Epidemiology 11, 720–727. https://www.jstor.org/stable/3703831.

Gong, T., Sun, Z., Zhang, X., Zhang, Y., Wang, S., Han, L., et al., 2019. Associations of black carbon and $PM_{2.5}$ with daily cardiovascular mortality in Beijing, China. Atmos. Environ. 214, 116876 https://doi.org/10.1016/j.atmosenv.2019.116876.

Guo, J.P., Zhang, X.Y., Che, H.Z., Gong, S.L., An, X., Cao, C.X., et al., 2009. Correlation between PM concentrations and aerosol optical depth in eastern China. Atmos. Environ. 43, 5876–5886. https://doi.org/10.1016/j.atmosenv.2009.08.026.

Haley, V.B., Talbot, T.O., Felton, H.D., 2009. Surveillance of the short-term impact of fine particle air pollution on cardiovascular disease hospitalizations in New York State. Environ. Health 8, 42. https://doi.org/10.1186/1476-069X-8-42.

Hall, E.S., 2018. Temporal-spatial ambient concentrator estimator (T-SpACE). Hierarchical Bayesian Model Software Used to Estimate Ambient Concentrations of NAAQS Air Pollutants in Support of Health Studies. United States Environmental Protection Agency, Washington, DC. EPA/600/R-18/01, 2018. https://cfpub.epa.gov/si/si_public_record_report.cfm?Lab=NERL&dirEntryId=339714. (Accessed 30 September 2020).

Han, W., Li, Z., Guo, J., Su, T., Chen, T., Wei, J., et al., 2020. The urban-rural heterogeneity of air pollution in 35 metropolitan regions across China. Rem. Sens. 12, 2320. https://doi.org/10.3390/rs12142320.

Hennekens, C.H., Buring, J.E., 1987. Epidemiology in Medicine. Little, Brown, and Company, Boston, ISBN 0-316-35636-0.

Hosmer Jr., D.W., Lemeshow, S., Sturdivant, R.X., 2013. Applied Logistic Regression, third ed. John Wiley & Sons, Inc., Hoboken, New Jersey, ISBN 978-0-470-58247-3.

HSCRC (Maryland Health Services Cost Review Commission), 2020. Available online at: https://hscrc.maryland.gov. (Accessed 30 September 2020).

Hu, X., Waller, L.A., Lyapustin, A., Wang, Y., Liu, Y., 2014. 10-year spatial and temporal trends of $PM_{2.5}$ concentrations in the southeastern US estimated using high-resolution satellite data. Amos. Chem. Phys. 14, 6301–6314. https://doi.org/10.5194/acp-14-6301-2014.

Hu, Z., 2009. Spatial analysis of MODIS aerosol optical depth, $PM_{2.5}$, and chronic coronary heart disease. Int. J. Health Geogr. 8, 27. https://doi.org/10.1186/1476-072X-8-27.

Hu, Z., Rao, K.R., 2009. Particulate air pollution and chronic ischemic heart disease in the eastern United States: a county-level ecological study using satellite aerosol data. Environ. Health 8, 26. https://doi.org/10.1186/1476-069X-8-26.

Hughes, J.S., 2017. Should the positive predictive value be used to validate complications measures? Med. Care 55, 87. https://doi.org/10.1097/MLR.0000000000000672.

Jin, Q., Crippa, P., Pryor, S.C., 2020. Spatial characteristics and temporal evolution of the relationship between $PM_{2.5}$ and aerosol optical depth over the eastern USA during 2003-2007. Atmos. Environ. 239, 117718 https://doi.org/10.1016/j.atmosenv.2020.117718.

Kelsey, J.L., Whittemore, A.S., Evans, A.S., Thompson, W.D., 1996. Methods in Observational Epidemiology, second ed. Oxford University Press, New York, ISBN 0-19-508377-6.

Khalili, R., Bartell, S.M., Hu, X., Liu, Y., Chang, H.H., Belanoff, C., et al., 2018. Early-life exposure to $PM_{2.5}$ and risk of acute asthma clinical encounters among children in Massachusetts: a case-crossover analysis. Environ. Health 17, 20. https://doi.org/10.1186/s12940-018-0361-6.

Kim, H., Kim, J., Kim, S., Kang, S.H., Kim, H.J., Kim, H., et al., 2017. Cardiovascular effects of long-term exposure to air pollution: a population-based study with 900 845 Person-Years of follow-up. J. Am. Heart Assoc. 6, e007170 https://doi.org/10.1161/JAHA.117.007170.

Kloog, I., Chudnovsky, A.A., Just, A.C., Nordico, F., Koutrakis, P., Coull, B.A., et al., 2014a. A new hybrid spatio-temporal model for estimating daily multi-year $PM_{2.5}$ concentrations across Northeastern USA using high resolution aerosol optical depth data. Atmos. Environ. 95, 581–590. https://doi.org/10.1016/j.atmosenv.2014.07.014.

Kloog, I., Coull, B.A., Zanobetti, A., Koutrakis, P., Schwartz, J.D., 2012a. Acute and chronic effects of particles on hospital admissions in New England. PloS One 7, e34664. https://doi.org/10.1371/journal.pone.0034664.

Kloog, I., Nordio, F., Coull, B.A., Schwartz, J., 2012b. Incorporating local land use regression and satellite aerosol optical depth in a hybrid model of spatio-temporal $PM_{2.5}$ exposures in the Mid-Atlantic states. Environ. Sci. Technol. 46, 11913–11921. https://doi.org/10.1021/es302673e.

Kloog, I., Nordio, F., Zanobetti, A., Coull, B.A., Koutrakis, P., Schwartz, J.D., 2014b. *S*hort *t*erm *e*ffects *o*f *p*article *e*xposure *o*n *h*ospital *a*dmissions *i*n *t*he *M*id-Atlantic *s*tates: a *p*opulation *e*stimate. *P*loS One 9, e88578. https://doi.org/10.1371/journal.pone.0088578.

Kumar, N., Chu, A., Foster, A., 2007. An empirical relationship between $PM_{2.5}$ and aerosol optical depth in Delhi Metropolitan. Atmos. Environ. 41, 4492–4503. https://doi.org/10.1016/j.atmosenv.2007.01.046.

Kumar, N., Liang, D., Comellas, A., Chu, A.D., Abrams, T., 2013. Satellite-based PM concentrations and their application to COPD in Cleveland, OH. J. Expo. Sci. Environ. Epidemiol. 23, 637–646. https://doi.org/10.1038/jes.2013.52.

Kumar, R., 2016. Evaluation of diagnostic tests. Clin. Epidemiol. Glob. Health 4, 76–79. https://doi.org/10.1016/j.cegh.2015.12.001.

Last, J.M., 1995. A Dictionary of Epidemiology, third ed. Oxford University Press, New York, ISBN 0-19-509668-1.

Lee, H.J., Coull, B.A., Bell, M.L., Koutrakis, P., 2012. Use of satellite-based aerosol optical depth and spatial clustering to predict ambient $PM_{2.5}$ concentrations. Environ. Res. 118, 8–15. https://doi.org/10.1016/j.envres.2012.06.011.

Lee, M., Kloog, I., Chudnovsky, A., Lyapustin, A., Wang, Y., Melly, S., et al., 2016a. Spatiotemporal prediction of fine particulate matter using high-resolution satellite images in the southeastern US 2003-2011. J. Expo. Sci. Environ. Epidemiol. 26, 377–384. https://doi.org/10.1038/jes.2015.41.

Lee, M., Koutrakis, P., Coull, B., Kloog, I., Schwartz, J., 2016b. Acute effect of fine particulate matter on mortality in three Southeastern states from 2007-2011. J. Expo. Sci. Environ. Epidemiol. 26, 173–179. https://doi.org/10.1038/jes.2015.47.

Li, J., Carlson, B.E., Lacis, A.A., 2015. How well do satellite AOD observations represent the spatial and temporal variability of $PM_{2.5}$ concentration for the United States? Atmos. Environ. 102, 260–273. https://doi.org/10.1016/j.atmosenv.2014.12.010.

Liu, C.J., Liu, C.Y., Mong, N.T., Chou, C.C.K., 2016. Spatial correlation of satellite-derived $PM_{2.5}$ with hospital admissions for respiratory diseases. Rem. Sens. 8, 914. https://doi.org/10.3390/rs8110914.

Liu, Y., Sarnat, J.A., Kilaru, V., Jacob, D.J., Koutrakis, P., 2005. Estimating ground-level $PM_{2.5}$ in the Eastern United States using satellite remote sensing. Environ. Sci. Technol. 39, 3269–3278. https://doi.org/10.1021/es049352m.

Ma, Y., Yang, S., Yu, Z., Jiao, H., Zhang, Y., Ma, B., 2019. A study of the short-term impact of fine particulate matter pollution on the incidence of cardiovascular diseases in Beijing, China. Atmos. Environ. 215, 116889 https://doi.org/10.1016/j.atmosenv.2019.116889.

Ma, Z., Hu, X., Sayer, A.M., Levy, R., Zhang, Q., Xue, Y., et al., 2016. Satellite-based spatiotemporal trends in $PM_{2.5}$ concentrations: China, 2004-2013. Environ. Health Perspect. 124, 184–192. https://doi.org/10.1289/ehp.1409481.

Maclure, M., 1991. The case-crossover design: a method for studying transient effects on the risk of acute events. Am. J. Epidemiol. 133, 144–153. https://doi.org/10.1093/oxfordjournals.aje.a115853.

Madrigano, J., Kloog, I., Goldberg, R., Coull, B.A., Mittleman, M.A., Schwartz, J., 2013. Long-term exposure to $PM_{2.5}$ and incidence of acute myocardial infarction. Environ. Health Perspect. 121, 192–196. https://doi.org/10.1289/ehp.1205284.

McGuinn, L.A., Ward-Caviness, C.K., Neas, L.M., Schneider, A., Diaz-Sanchez, D., Cascio, W.E., et al., 2016. Association between satellite-based estimates of long-term $PM_{2.5}$ exposure and coronary artery disease. Environ. Res. 145, 9–17. https://doi.org/10.1016/j.envres.2015.10.026.

McMillan, N.J., Holland, D.M., Morara, M., Feng, J., 2010. Combining numerical model output and particulate data using Bayesian space-time modeling. Environmetrics 21, 48–65. https://doi.org/10.1002/env.984.

MDH (Maryland Department of Health), 2021. Institutional Review Board. Available online at. https://health.maryland.gov/oig/irb/Pages/IRB.aspx. (Accessed 25 July 2021).

MDP (Maryland Department of Planning), 2020. Maryland State Data Center, Zip Code Boundary Area Files, 2004 and 2006. Available online at: http://planning.maryland.gov/MSDC/Pages/s5_map_gis.aspx. (Accessed 30 September 2020).

NCEI (National Centers for Environmental Information), 2020. Climate Data Online. Available online at: https://www.ncdc.noaa.gov/cdo-web/. (Accessed 30 September 2020).

NOAA (National Oceanic and Atmospheric Administration), 2020. The New Improved "Wind Chill Index. Available online at: https://www.weather.gov/ffc/wci. (Accessed 30 September 2020).

Norris, G., YoungPong, S.N., Koenig, J.Q., Larson, T.V., Sheppard, L., Stout, J.W., 1999. An association between fine particles and asthma emergency department visits for children in Seattle. Environ. Health Perspect. 107, 489–493. https://doi.org/10.1289/ehp.99107489.

OPM (US Office of Personnel Management), 2020. Federal Holidays, 2004–2006. Available online at: https://archive.opm.gov/Operating_Status_Schedules/fedhol/2004.asp. (Accessed 30 September 2020).

Peters, A., Dockery, D.W., Muller, J.E., Mittleman, M.A., 2001. *I*ncreased *p*articulate air *p*ollution *a*nd *t*he *t*riggering *o*f *m*yocardial *i*nfarction. *C*irculation 103, *2*810–2815. https://doi.org/10.1161/01.cir.103.23.2810.

Prud'homme, G., Dobbin, N.A., Sun, L., Burnett, R.T., Martin, R.V., Davidson, A., et al., 2013. Comparison of remote sensing and fixed-site monitoring approaches for examining air pollution and health in a national study population. Atmos. Environ. 80, 161–171. https://doi.org/10.1016/j.atmosenv.2013.07.020.

Qiu, H., Yu, I.T.S., Wang, X., Tian, L., Tse, L.A., Wong, T.W., 2013. Differential effects of fine and coarse particles on daily emergency cardiovascular hospitalizations in Hong Kong. Atmos. Environ. 64, 296–302. https://doi.org/10.1016/j.atmosenv.2012.09.060.

Rodopoulou, S., Samoli, E., Chalbot, M.C.G., Kavouras, I.G., 2015. Air pollution and cardiovascular and respiratory emergency visits in Central Arkansas: *a* time series analysis. Sci. Total Environ. 536, 872–879. https://doi.org/10.1016/j.scitotenv.2015.06.056.

Rosamond, W.D., Chambless, L.E., Sorlie, P.D., Bell, E.M., Weitzman, S., Smith, J.C., et al., 2004. Trends in the sensitivity, positive predictive value, false-positive rate, and comparability ratio of hospital discharge diagnosis codes for acute myocardial infarction in four US communities, 1987-2000. Am. J. Epidemiol. 160, 1137–1146. https://doi.org/10.1093/aje/kwh341.

Rothfusz, L.P., 2020. The Heat Index "Equation," SR-90-23, 7/1/90. Available online at: https://www.weather.gov/media/ffc/ta_htindx.PDF. (Accessed 30 September 2020).

SAS (Statistical Analysis System), 2017. Base SAS 9.4. In: seventh ed. SAS (Statistical Analysis System), 2018. SAS/STAT 15.1 User's Guide: High-Performance Procedures, SAS Institute Inc. SAS Institute Inc., Cary, NC (Cary, NC).

Schlesselman, J.J., 1982. Case-Control Studies: Design, Conduct, Analysis. Oxford University Press, New York, ISBN 0-19-502933-X.

Sorek-Hamer, M., Just, A.C., Kloog, I., 2016. Satellite remote sensing in epidemiological studies. Curr. Opin. Pediatr. 28, 228–234. https://doi.org/10.1097/MOP.0000000000000326.

Stokes, M.E., Davis, C.S., Koch, G.G., 2012. Categorical Data Analysis Using SAS, third ed. SAS Institute Inc., Cary, NC, ISBN 978-1-61290-090-2.

Strickland, M.J., Hao, H., Hu, X., Chang, H.H., Darrow, L.A., Liu, Y., 2016. Pediatric emergency visits and short-term changes in $PM_{2.5}$ concentrations in the US state of Georgia. Environ. Health Perspect. 124, 690–696. https://doi.org/10.1289/ehp.1509856.

Szyszkowicz, M., Kousha, T., Castner, J., Dales, R., 2018. Air pollution and emergency department visits for respiratory diseases: a multi-city case-crossover study. Environ. Res. 163, 263–269. https://doi.org/10.1016/j.envres.2018.01.043.

Tapia, V., Steenland, K., Sarnat, S.E., Vu, B., Liu, Y., Sánchez-Ccoyllo, O., et al., 2020. Time-series analysis of $PM_{2.5}$ and cardiorespiratory emergency room visits in Lima, Peru during 2010-2016. J. Expo. Sci. Environ. Epidemiol. 30, 680–688. https://doi.org/10.1038/s41370-019-0189-3.

Tétreault, L.F., Doucet, M., Gamache, P., Fournier, M., Brand, A., Kosatsky, T., et al., 2016. *C*hildhood *e*xposure *to t*he *a*mbient *a*ir *p*ollutants *a*nd *t*he *o*nset *of a*sthma: *an a*dministrative *c*ohort *s*tudy *in Q*uébec. *E*nviron. Health Perspect. 124, *1*276–1282. https://doi.org/10.1289/ehp.1509838.

Tsai, S.S., Chang, C.C., Yang, C.Y., 2013. Fine particulate air pollution and hospital admissions for chronic obstructive pulmonary disease: a case-crossover study in Taipei. Int. J. Environ. Res. Publ. Health 10, 6015–6026. https://doi.org/10.3390/ijerph10116015.

USCB (US Census Bureau/Department of Commerce), 2020. 2000 Census of People and Housing, Summary File 3. Available online at: https://www.census.gov/data/datasets/2000/dec/summary-file-3.html. (Accessed 30 September 2020).

van Donkelaar, A., Martin, R.V., Brauer, M., Boys, B.L., 2015. Use of satellite observations for long-term exposure assessment of global concentrations of fine particulate matter. Environ. Health Perspect. 123, 135–143. https://doi.org/10.1289/ehp.1408646.

van Donkelaar, A., Martin, R.V., Brauer, M., Kahn, R., Levy, R., Verduzco, C., et al., 2010. Global estimates of ambient fine particulate matter concentrations from satellite-based aerosol optical depth: development and application. Environ. Health Perspect. 118, 847–855. https://doi.org/10.1289/ehp.0901623.

Vu, B.N., Sánchez, O., Bi, J., Xiao, Q., Hansel, N.N., Checkley, W., et al., 2019. Developing an advanced $PM_{2.5}$ exposure model in Lima, Peru. Rem. Sens. 11, 641. https://doi.org/10.3390/rs11060641.

Wang, B., Chen, Z., 2016. High-resolution satellite-based analysis of ground-level $PM_{2.5}$ for the city of Montreal. Sci. Total Environ. 541, 1059–1069. https://doi.org/10.1016/j.scitotenv.2015.10.024.

Wang, C., Feng, L., Chen, K., 2019. The impact of ambient particulate matter on hospital outpatient visits for respiratory and circulatory system disease in an urban Chinese population. Sci. Total Environ. 666, 672–679. https://doi.org/10.1016/j.scitotenv.2019.02.256.

Wang, J., Yin, Q., Tong, S., Ren, Z., Hu, M., Zhang, H., 2017. Prolonged continuous exposure to high fine particulate matter associated with cardiovascular and respiratory disease mortality in Beijing, China. Atmos. Environ. 168, 1–7. https://doi.org/10.1016/j.atmosenv.2017.08.060.

Weber, S.A., Engel-Cox, J.A., Hoff, R.M., Prados, A.I., Zhang, H., 2010. An improved method for estimating surface fine particle concentrations using seasonally adjusted satellite aerosol optical depth. J. Air Waste Manag. Assoc. 60, 574–585. https://doi.org/10.3155/1047-3289.60.5.574.

Weber, S.A., Insaf, T.Z., Hall, E.S., Talbot, T.O., Huff, A.K., 2016. Assessing the impact of fine particulate matter ($PM_{2.5}$) on respiratory-cardiovascular chronic diseases in the New York City Metropolitan area using Hierarchical Bayesian Model estimates. Environ. Res. 151, 399–409. https://doi.org/10.1016/j.envres.2016.07.012.

Wu, Y., Li, M., Tian, Y., Cao, Y., Song, J., Huang, Z., et al., 2019. *S*hort-term *e*ffects *o*f ambient *f*ine *p*articulate *a*ir *p*ollution *on i*npatient *v*isits *f*or *m*yocardial *i*nfarction *in B*eijing, *C*hina. *E*nviron. Sci. Pollut. Res. Int. 26, *1*4178–14183. https://doi.org/10.1007/s11356-019-04728-8.

Xia, X., Yao, L., 2019. Spatio-temporal differences in health effect of ambient $PM_{2.5}$ pollution on acute respiratory infection between children and adults. IEEE Access 7, 25718–25726. https://doi.org/10.1109/ACCESS.2019.2900539.

Xie, Y., Wang, Y., Bilal, M., Dong, W., 2019. Mapping daily $PM_{2.5}$ at 500 m resolution over Beijing with improved hazy day performance. Sci. Total Environ. 659, 410–418. https://doi.org/10.1016/j.scitotenv.2018.12.365.

Xue, T., Zheng, Y., Geng, G., Zheng, B., Jiang, X., Zhang, Q., et al., 2017. Fusing observational, satellite remote sensing, and air quality model simulated data to estimate spatiotemporal variations of $PM_{2.5}$ exposure in China. Rem. Sens. 9, 221. https://doi.org/10.3390/rs9030221.

Yanosky, J.D., Paciorek, C.J., Laden, F., Hart, J.E., Puett, R.C., Liao, D., et al., 2014. Spatio-temporal modeling of particulate air pollution in the conterminous United States using geographic and meteorological predictors. Environ. Health 13, 63. http://www.ehjournal.net/content/13/1/63.

Yu, W., Liu, S., Jiang, J., Chen, G., Luo, H., Fu, Y., et al., 2020. Burden of ischemic heart disease and stroke attributable to exposure to atmospheric $PM_{2.5}$ in Hubei province, China. Atmos. Environ. 221, 117079 https://doi.org/10.1016/j.atmosenv.2019.117079.

Yu, Y., Yao, S., Dong, H., Ji, M., Chen, Z., Li, G., et al., 2018. Short-term effects of ambient air pollutants and myocardial infarction in Changzhou, China. Environ. Sci. Pollut. Res. 25, 22285–22293. https://doi.org/10.1007/s11356-018-2250-5.

Zhang, H., Hoff, R.M., Engel-Cox, J.A., 2009. The relation between moderate resolution imaging spectroradiometer (MODIS) aerosol optical depth and $PM_{2.5}$ over the United States: a geographical comparison by US environmental protection agency regions. J. Air Waste Manag. Assoc. 59, 1358–1369. https://doi.org/10.3155/1047-3289.59.11.1358.